Remote Sensing Research in Support of Archaeological Investigations at Four Localities on the Mississippi Gulf Coast

By Jay K. Johnson, Bryan S. Haley, and Edward R. Henry

Remote Sensing Research in Support of Archaeological Investigations at Four Localities on the Mississippi Gulf Coast

By Jay K. Johnson, Bryan S. Haley, and Edward R. Henry

Archaeological Report No. 38

Mississippi Department of Archives and History

Katie Blount
Director

Pamela Edwards Lieb
Series Editor

Chris Goodwin
Managing Editor

Gregory A. Waselkov
and Bonnie L. Gums
Technical Editors

Sarah B. Mattics
Design and Layout

Cover Illustration: GPR survey at 22JA633 of Grand Bay Estuary,
view to the south.

MISSISSIPPI Department *of*
MDA&H
ARCHIVES & HISTORY

Table of Contents

List of Figures

List of Tables

Acknowledgments

Introduction

In the aftermath of Hurricane Katrina, cultural resource managers found that their ability to respond to the immediate disaster, and to the continuing threats to archaeological sites posed by the recovery, was hampered by the fact that we know so little about the archaeology of the Mississippi Gulf coast. As a consequence, the Mississippi Department of Archives and History (MDAH) made use of grants from the US Department of Housing and Urban Development and Mississippi Development Authority to fund four major archaeological projects on the coast.

These research projects were designed to examine broad aspects of the coastal archaeological record. As part of this overall effort, a team of specialists from the Center for Archaeological Research at the University of Mississippi received a fifth grant to conduct remote sensing research in the other four locations to provide data that would be useful to the excavators. This remote sensing project was designed in consultation with the archaeologists who were responsible for each of the other projects. As described in the following chapters, each remote sensing exercise was designed to take into account survey conditions, as well as broader project goals. Instrumentation ranged from satellite to airborne to a variety of geophysical remote sensing instruments, each of which is suited to recording different specific aspects of the archaeological record.

Grand Bay Shell Middens

The extensive marshlands located between Pascagoula, Mississippi and the Alabama state line contain several recorded shell middens, although the area has never been examined systematically. Grand Bay encompasses approximately 10,800 acres (43.7 square kilometers) of terrain that is difficult to navigate and evaluate using traditional survey techniques. However, because shell middens alter the elevation, drainage, and soil chemistry of the marsh, they have a distinctive spectral signature that is measurable by remote sensing technology (Giardino and Haley 2006; Marco Giardino, personal communication 2009). Therefore, as a first step in the evaluation of site location in the survey area, all known sites were visited and their locations accurately plotted by global positioning system (GPS). These data were compiled in a geographic information system (GIS) data base for analysis and future reference.

Fortunately, the University of Mississippi's remote sensing team has complete pre-Katrina (2002) high spatial resolution (sub-meter) satellite imagery with four-band spectral resolution of the Gulf coast, including the survey area, from DigitalGlobe, a commercial supplier of space imagery. Imagery data from DigitalGlobe's QuickBird satellite was coupled with digital elevation model data and GPS data to refine the locational data for archaeological sites in Grand Bay. Our spectral analysis is based on the QuickBird imagery.

In addition, we mapped a sample of the Grand Bay shell middens using ground-penetrating radar (GPR) to document both the horizontal and vertical distributions of shell in the middens. Because the shell middens are part of the Grand Bay National Wildlife Refuge, we could not clear the sites of vegetation and it was necessary to develop new procedures for recording GPR data.

La Pointe-Krebs Plantation, 22JA526

The La Pointe-Krebs Plantation site has been the subject of three previous archaeological investigations (Hinks et al. 1993; Waselkov and Silvia 1995; Gums 1996). The first two focused primarily on the immediate area of the La Pointe-Krebs house itself (perhaps the oldest standing structure in Mississippi), while the latest consisted of a comprehensive shovel test survey of the entire property. The archaeological record at this site includes an early historic Indian shell midden along with French, Spanish, and British colonial deposits, and more recent features and middens from the nineteenth and twentieth centuries. The site is presently a park (known as Old Spanish Fort Park) operated by Jackson County, although the park is no longer open to the public because of damage sustained by the old house during Hurricane Katrina.

The geophysical survey was comprehensive, covering the entire park area with GPR, gradiometry, and electromagnetic (EM) conductivity/magnetic susceptibility. From previous experience on colonial-era Chickasaw sites we have found gradiometer data in combination with EM data particularly useful in delineating the locations of midden pits. Our EM instrument measures soil conductivity and magnetic susceptibility simultaneously, and it is susceptibility data which allows us to evaluate gradiometer results

for likely midden deposit locations. We had intended to use the distribution of areas of high susceptibility to target possible midden areas, which would in turn be tested for depth and intensity using down-hole susceptibility. Unfortunately, for reasons that will be explored in depth in the following chapters, susceptibility does not appear to be useful in locating midden deposits in the sands of the Gulf coast.

Jackson Landing Site, 22HA504

Jackson Landing/Mulatto Bayou has been the subject of archaeological inquiry since the 19th century when the site was visited by B. L. C. Wailes (Williams 1987). Mark Williams conducted the first excavations of the site in 1972, concentrating his efforts on the east end of the earthworks. A shell midden at the edge of Mulatto Bayou was tested by Charles Pearson, Diane Wiseman, Marco Giardino, and Robert Jones (Weinstein 2009). Finally, a platform mound at the site was tested by Kelsey Lowe and Tony Boudreaux in 2007 (2008).

In spite of what, for coastal Mississippi, is an unusual amount of work, only a small fraction of the site has been investigated. In particular, the areas between the platform mound and the bayou and between the earthworks and the bayou have not been evaluated. We had intended to use geophysical survey instruments to explore these areas. Unfortunately, because of difficulty in negotiating a non-indemnity clause between the University of Mississippi and the corporation that owns the land, we were not able to do the remote sensing survey until after the excavations had been completed. Therefore, we focused on the mound and an area on the western bluff where excavation data could be used to evaluate the geophysical survey results, rather than the reverse as had been planned. We used GPR, gradiometry, EM, and down-hole susceptibility with some success at the Jackson Landing site.

Graveline Mound, 22JA503

This relatively small platform mound with a ramp has been known since C. B. Moore's investigations of the Gulf coast early in the 20th century and was tested by John Blitz and Baxter Mann in 1992 (Blitz and Mann 1993). Blitz and Mann's investigations included auger tests and one test pit on the eastern edge of the mound. Their excavations revealed seven distinct phases of mound construction, some of which showed evidence of habitation in the form of burned clay and midden. We postulated that if either the burning or the midden deposits were of sufficient magnitude, they would be detectable using GPR, gradiometry,

EM, and down-hole susceptibility. Given the relatively small size of the mound (30 by 25 m), we were able to provide total coverage with GPR and gradiometry and electrical resistivity tomography, and partial coverage with down-hole susceptibility. In addition, we generated a topographic map on the basis of elevational data gathered in setting up the grid used in the geophysical survey of the site.

Chapter 1
Grand Bay

The primary goal of initial fieldwork at Grand Bay, on the Mississippi Gulf coast, adjacent to Alabama, was to establish precise locations of known archaeological sites. This was an essential first step in the search for site signatures in satellite imagery. Subsequently, we conducted a multivariate analysis of satellite imagery and concluded with a ground penetrating radar (GPR) survey of selected sites.

Determining Site Locations

[Editor's Note: Because archaeological site security is a real concern these days, and the State of Mississippi is legally obligated to protect archaeological site location information, most of the accompanying figures have been removed from the following discussion. Professional archaeologists may request a fully illustrated version of this chapter from the State Archaeologist or from the senior author.]

Four sets of spatial data were integrated in refining site locations. We began with data from the Mississippi Department of Archives and History (MDAH) site file, which includes Universal Transverse Mercator (UTM) grid coordinates for site centroids and site polygons, as recorded on the Kreole, Miss.-Ala., and Grand Bay SW, Miss.-Ala., US Geological Survey 7.5´ series topographic quadrangle maps. The location of 22JA770 had not been recorded on the quadrangle maps and was taken from the site card. These site locational data were entered into a GIS relational database created in ArcMap 9.3.1, a geo-spatial processing program by ESRI.

The second data layer used in this research was a digital elevation model (DEM) downloaded from the Mississippi Automated Resource Information System (MARIS) web site <www.maris.state.ms.us/>. This DEM is based on airborne Light Detection and Ranging (LIDAR) data recorded with a 20-m horizontal resolution. Once processed, these data make possible the precise mapping of relative elevations within the marsh.

The third data layer is a QuickBird four-band satellite image of the research area. These data were recorded on August 29, 2002, exactly three years before Hurricane Katrina had a major impact on the Grand Bay marsh. The four scenes that make up the mosaic cover the entire survey area. Cloud cover is minimal in this image and largely restricted to the western portion of the survey area where sites have not been found.

The majority of known sites are located on and a short distance back from the shoreline of Point Aux Chenes Bay. It is useful to focus on this area in the following discussion. Prior to fieldwork, MDAH site locations were digitized as a layer in the master Grand Bay GIS and exported as tracks to a handheld GPS using the DNRGarmin add on. The Garmin GPS 76csx instrument we used had a base map showing bayous, shorelines, and other landscape features. It was therefore quite easy to locate known sites and evaluate prior locational data. Site boundaries were then recorded more precisely by taking GPS readings at the shoreline limits of each shell midden.

The final set of locational data to be considered comprised site locations recorded during a post-Hurricane Katrina assessment project (Boudreaux 2009). Site boundaries had been mapped during that project

Figure 1-1. Banks Island, Bayou Cumbest area, QuickBird imagery.

with a field laptop computer linked to a portable GPS (Boudreaux 2009: Figures 4.4 and 4.5). Coastal Environments Inc. (CEI) provided Grand Bay site polygons as shapefiles to be added directly to the GIS. While there was general agreement between the MDAH, post-Katrina assessment, and CEI site locations, in almost all cases, actual site limits were smaller than previously recorded limits. In a few cases recorded site locations were difficult to reconcile with their actual locations. In a few notable situations, sites had been dramatically modified by general erosion and, more specifically, by the impact of Katrina.

The effects of Katrina are most evident at the mouth of Bayou Cumbest, especially in the case of 22JA632 and 22JA634. The Grand Bay SW, Miss.-Ala., and the Kreole, Miss.-Ala., USGS topographic quadrangle maps were among the first 7.5′ series maps issued for the State of Mississippi; both are based on aerial photos taken in 1952. Considerable erosion is evident by comparing, for example, Bangs Island as represented on the quadrangle map and on the 2002 QuickBird

imagery (Figure 1-1). Another measure of erosion taking place at the mouth of Bayou Cumbest is the strong reflectance in all bands of the QuickBird imagery (white in Figure 1-1) caused by the exposed and wave-washed shells that mark the locations of sites 22JA632 and 22JA634 (Figure 1-2). In fact, Katrina appears to have redeposited a substantial portion of 22JA632 in the marsh to the north (Figure 1-3).

Taking advantage of the fact that vegetation had been completely scoured from the surface of site 22JA632, we ran north-south and east-west GPR transects across the site surface (Figure 1-4). Preliminary results suggested we could easily detect and measure the boundary between shells and sand that marks the lower limit of the shell deposit.

In addition to mapping the distribution of exposed shells, the QuickBird sensor makes it easy to distinguish trees from marsh, since trees show up as bright red in the imagery (see Figure 1-1), because chlorophyll in tree leaves is a strong near-infrared (IR) reflector and that wavelength band has been assigned the color red on the display. There is a direct correspondence between the locations of trees and the slight elevations selected for human habitation (Figure 1-5). In this image, relative elevation is emphasized by passing a large window filter through the DEM data, a filtering process called detrending that removes large scale trends in the data. In this case, we detrended the general increase in elevation that occurs as you move away from the Gulf, which makes local variation in elevation more easily detected.

Of the three Bayou Cumbest sites, the 22JA632 and 22JA634 locations needed correction as a result of shoreline modification resulting from general erosion and the effects of Katrina. Also, both the CEI and post-Katrina assessment data shifted 22JA633 to the east, occupying the extreme eastern end of the ele-

Figure 1-2. Southern edge of 22JA632, view to the west.

Figure 1-3. Northern edge of 22JA632, shell deposits relocated by storm surge.

Figure 1-4. GPR survey at 22JA632, view to the north.

vation upon which it is in fact located. We ran one north-south GPR transect across 22JA633, which gave relatively poor results (Figure 1-6).

The greatest discrepancy between site locations recorded on USGS quadrangle maps and actual site locations occurs on the east shore of L'Isle Chaude Bay. This is likely the result of the fact that these sites were recorded relatively early, well before the general use of GPS equipment. Of the three northernmost site locations, only one, 22JA581 (as recorded in the site files), coincides with a site. There are actually three small shell midden deposits in the general area of the original site locations (Figure 1-7) and another large shell midden to the south. The southern midden is evident on the quadrangle map and the satellite imagery (Figure 1-8) as a tree-covered elevation (Figure 1-9). Following CEI, this was assigned site number 22JA582. That leaves two site numbers for three separate small shell deposits to the north. The northern one has been assigned 22JA580, while the middle two have been arbitrarily called 22JA581a and 22JA581b. Once again, the exposed shells at the southern end of L'Isle Chaude shows a strong reflectance marking the location of exposed shells of the 22JA710 midden (Figure 1-10).

Like nearly all of the revised site locations, 22JA587 is mapped much smaller than originally recorded. According to the site file location, it covered both banks of a narrow peninsula of land created by a sharp bend in Crooked Bayou. There are, in fact, tree-covered elevations on both banks (see Figure 1-8). However, archaeological deposits are only evident on the south bank. This area will be particularly useful in developing a site signature based on vegetation that can discriminate these two, nearby tree-covered hammocks. The most prominent elevation in this area is that occupied by 22JA582 and a single GPR transect at this site produced promising results (Figure 1-11).

Site 22JA770 was first recorded by CEI in their post-Katrina survey and is represented on the site file card by a large generalized oval that is clearly too large. QuickBird imagery shows a small clump of trees within the boundaries of the site card polygon, and there is also a slight elevation evident on the LIDAR data (Fig-

Figure 1-6. GPR survey at 22JA633, view to the south.

Figure 1-5. Banks Island, Bayou Combest area, LIDAR imagery.

Figure 1-7. Southern end of 22JA581 with 22JA582 in the background, view to the south.

Table 1-1. Unsupervised Classification Results for 10, 15, and 20 Classes.

10 Classes		15 Classes		20 Classes	
Ground Truth	**Pixels**	**Ground Truth**	**Pixels**	**Ground Truth**	**Pixels**
		Bare Marsh	81,028	Bare Marsh	42,662
Bare Marsh/ Cloud	171,407	Bare Marsh/ Cloud	112,723	Bare Marsh/ Cloud	65,738
				Bare Marsh/Cloud	68,359
Cloud	104,559	Cloud	81,684	Cloud	80,261
Cloud	117,103	Cloud	90,318	Cloud	76,137
				Cloud	86,508
Cloud Shadow	137,512	Cloud Shadow	83,753	Cloud Shadow	44,326
		Cloud Shadow	98,808	Cloud Shadow	56,583
Hammock	302,145	Hammock	363,320	Hammock	350,374
		Hammock	181,928	Hammock	171,570
Marsh	2,530,853	Marsh	461,409	Marsh	113,758
		Marsh	1,044,266	Marsh	691,173
		Marsh	923,306	Marsh	692,460
				Marsh	960,386
Water	88,732	Water	195,548	Water	60,280
Water	535,768	Water	451,023	Water	218,360
Water	254,146	Water	1,121,705	Water	341,323
Water	1,355,118	Water	306,524	Water	767,226
				Water	668,263
				Water/Cloud	41,596

Figure 1-8. Jose Bay area, QuickBird imagery.

Figure 1-9. 22JA582, view to the south.

ure 1-12). Interestingly, site 22JA770 is located more than 370 m from Bayou Heron, the major waterway in the area (Figure 1-13), and more than 100 m from a small unnamed drainage that is today much too small to be navigated, even by canoe. Closer views of the 22JA770 area show a small elevation in the DEM data and a clump of trees at that same spot. A GPS track walked around the boundary of the site corresponds almost exactly with this clump of trees (Figure 1-14). The correspondence is certainly within the error level of a handheld GPS unit.

Site 22JA771 was relocated to the south of its original location, as well as south of the CEI location on the basis of GPS readings. Our GPS points, which were taken along the shoreline, are located nearly 20 m inland. However, an examination of the satellite imagery shows that the outside bend of the bayou has migrated in the several decades since 1952, when the aerial photographs were taken upon which the Kreole quadrangle map was based. The QuickBird image also shows the clump of trees that mark the location of this site.

Site 22JA562 could not be relocated. The CEI surveyors noted this site was completely submerged. "The portions of the submerged, redeposited shell that represent the remains of the site are actually located in Alabama" (Boudreaux 2009:152).

A couple of things become evident in this initial review of site locations within the Grand Bay marsh. First, except for a few sites located along the southern edge of the marsh, the shell middens are located on distinct elevations. It may be that the bay front sites were elevated, but have been completely deflated as a result of hundreds of years of storm damage. To some extent, the site elevations are created by the accumulation of shells during the course of site occupation. Some of the elevations seem to be solely the result of this accumulation, but some are not. There are several well-defined elevations, particularly along Bayou Cumbest, which do not appear to have been occupied or were only partially occupied. Bayou Cumbest is especially interesting because it clearly originated as a meandering river that once had a much larger drainage. The Bayou Cumbest elevations can be related to natural levee deposition during the period when that

Figure 1-10. 22JA710, view to the east.

Figure 1-11. GPR survey at 22JA582, view to the south.

Figure 1-12. Bayou Heron area, QuickBird imagery.

Table 1-2. Class Pixel Composition of Three Sites.

Class	Survey Area		22JA633		22JA575		22JA582	
	Pixels	Prop.	Pixels	Prop.	Pixels	Prop.	Pixels	Prop.
Bare Marsh	81,028	0.01	0	0.00	0	0.00	0	0.00
Bare Marsh/Cloud	112,723	0.02	0	0.00	0	0.00	1	0.01
Cloud	81,684	0.01	0	0.00	0	0.00	0	0.00
Cloud	90,318	0.02	0	0.00	0	0.00	0	0.00
Cloud Shadow	83,753	0.01	0	0.00	0	0.00	0	0.00
Cloud Shadow	98,808	0.02	0	0.00	0	0.00	0	0.00
Hammock	363,320	0.06	142	0.21	457	0.89	115	0.61
Hammock	181,928	0.03	508	0.76	24	0.05	50	0.26
Marsh	461,409	0.08	0	0.00	0	0.00	7	0.04
Marsh	1,044,266	0.19	14	0.02	1	0.00	8	0.04
Marsh	923,306	0.16	2	0.00	31	0.06	9	0.05
Water	195,548	0.03	0	0.00	0	0.00	0	0.00
Water	451,023	0.08	0	0.00	0	0.00	0	0.00
Water	1,121,705	0.20	0	0.00	0	0.00	0	0.00
Water	306,524	0.05	0	0.00	0	0.00	0	0.00
Total	5,597,343		666		513		190	

Table 1-3. Distance Statistics Based on 22JA633 Signature.

Area	Min.	Max.	Mean	S.D.	n
22JA633	0.000	34.030	3.114	3.039	666
22JA633 Hammock	0.000	34.030	3.296	2.510	10528
22JA582	0.000	14.838	3.742	3.289	190
22JA575	0.000	25.639	3.076	3.475	513

Table 1-4. Distance Statistics Based on 22JA587 Signature.

Area	Min.	Max.	Mean	S.D.	n
22JA582	0.000	14.315	3.112	2.923	190
22JA582 Hammock	0.000	35.355	2.591	3.076	1591

drainage carried a much higher sediment load. There are likely some very old surfaces along this bayou.

Elevations in the marsh that support trees and other distinctive vegetation are known as hammocks in north Florida. Which brings us to our second point, that, upon initial observation, it is difficult to distinguish between hammocks of live oaks, yucca, and cactus that cover shell deposits and those which do not. Two site locations make this point well. Site 22JA582 is located on a low elevation on the interior of a sharp bend in Bayou Rigolets. A similar elevation covered with similar vegetation is located less than 100 m to the north, on the other side of the bend, with no evident archaeological deposit there. Site 22JA633 occupies only the eastern end of one of the natural levees on Bayou Cumbest, all of which is covered with live oaks and associated vegetation. Once again, there is no apparent difference in vegetation between where the site is located and where it is not.

Satellite Image Analysis

Another primary goal of remote sensing research in Grand Bay was the search for a satellite imagery

spectral signature that would identify site locations. The QuickBird imagery used in the following analysis was recorded on August 29, 2002, with a spatial resolution of 2.8 m for four bands, including blue (450-520 nm), green (520-600 nm), red (630-690 nm), and near-IR (760-900 nm). To translate, the specific spectral values for these four bands of energy were recorded for each pixel (picture element) in the scene and each pixel measured 2.8 m on a side. These are excellent images; the few small clouds do not affect the analysis, since neither the clouds nor their shadows fall on any of the known site locations. As a first step, four scenes were joined using the mosaic function in ArcMap (Figure 1-15), creating a scene 4,096 pixels square. The data set therefore amounts to more than 67 million pieces of information ($4,096^2$ x 4). In order to restrict the analysis to include just the Grand Bay marshes, ERDAS IMAGINE 9.3 software was used to subsample the image (Figure 1-16) and for all of the following image analysis. GIS analysis was performed in ArcMap.

There are two basic types of image classification, supervised and unsupervised. In an unsupervised analysis, statistically similar clusters of pixels are identified. The result is an image in which each pixel has been reclassified into one of the classes identi-

fied in the analysis. This is an excellent technique to explore the spectral characteristics of an image. Major land cover classes will generally be detected. In a supervised classification, the user specifies areas or groups of pixels within a scene that are known to have special characteristics of interest. Each of the pixels in the scene is then classified and evaluated as to the likelihood they belong to the signature generated to characterize the specified areas.

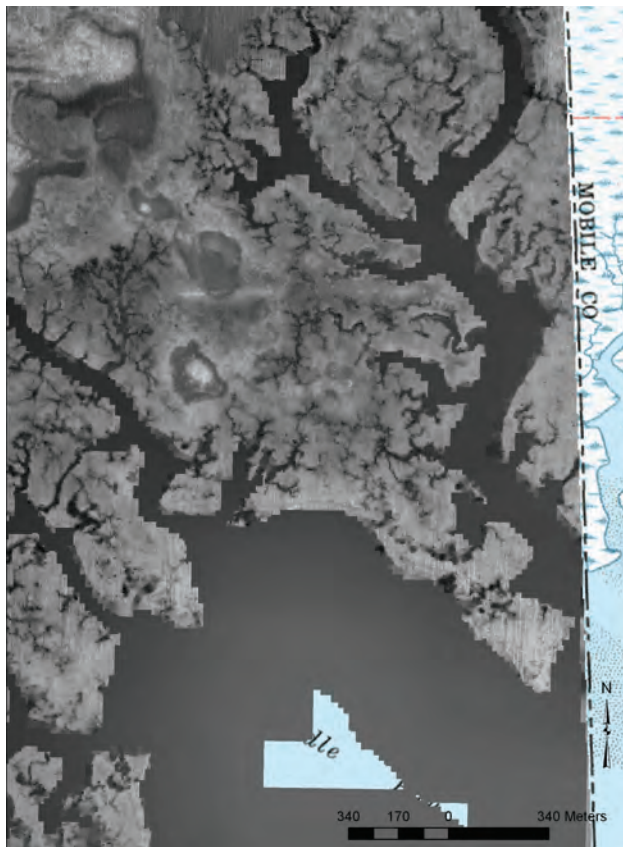**Figure 1-14.** Crossing the marsh to 22JA770, view to the northwest.

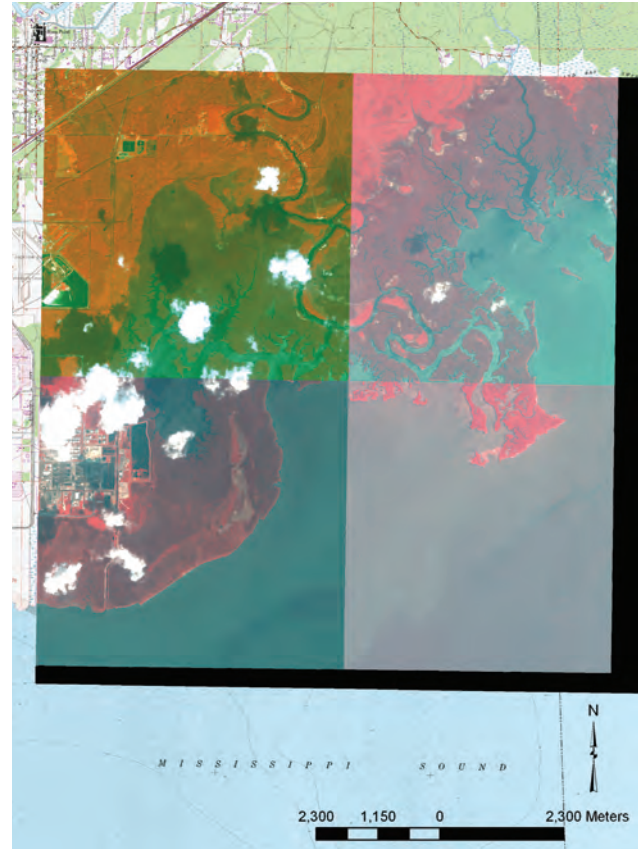**Figure 1-13.** Bayou Heron area, LIDAR imagery.

Figure 1-15. Mosaic of four QuickBird scenes covering the survey area.

As a first step in the Grand Bay analysis, we ran an unsupervised classification. In situations where the signature class for the area of interest is particularly distinct, it will often be detected using unsupervised techniques. At minimum, this approach provides a clear picture of the major dimension of variation in the scene and what that means for the analysis. The unsupervised process in ERDAS is iterative. Beginning with a user-specified number of classes to be produced, the program begins by calculating the specified number of arbitrary, evenly-spaced segments of spectral space. In this analysis, we began with 10 classes in a four-dimensional space. The program then calculates the mean value for each segment and computes the distance of each pixel to each mean, assigning the pixel to the class it most closely resembles. The means for the resulting clusters are then used to classify each pixel once again. The process continues until the percentage of pixels that were not reclassified in the latest iteration reaches a user-specified threshold—95 percent, in this analysis.

Three different unsupervised analyses were run with 10, 15, and 20 classes specified. The results reveal a good deal about the nature of the ground cover in the survey area (see Table 1-1). "Ground truth" class

assignments are based on a general knowledge of the survey area and an examination of the false color IR image (Figure 1-16). The 10-class solution is obviously the most concise, with all of the major land classes covered by one or more classes (Figure 1-17). Only two ground truth assignments, water and cloud, are represented by more than one class. Only one class, bare marsh/cloud, includes more than one ground truth assignment. The 15-class solution splits out a good many of the areas of bare marsh from the combined category. It also distinguishes two types of hammock vegetation and three types of marsh vegetation (Figure 1-18). However, the ambiguous bare marsh/cloud class persists. While the 20-class solution further subdivides both marsh vegetation and water, it adds a second bare marsh/cloud class and creates a second ambiguous class, water/cloud (Figure 1-19).

While a botanist with an integrated GIS/GPS could derive a good deal more information about these classifications through actual ground truth study in the field, the results are sufficient for our needs. In the first place, the classification is clearly responding to the two major areas of variation: marsh vegetation and water. Hammock vegetation, which is of greatest interest in the search for an archaeological site signa-
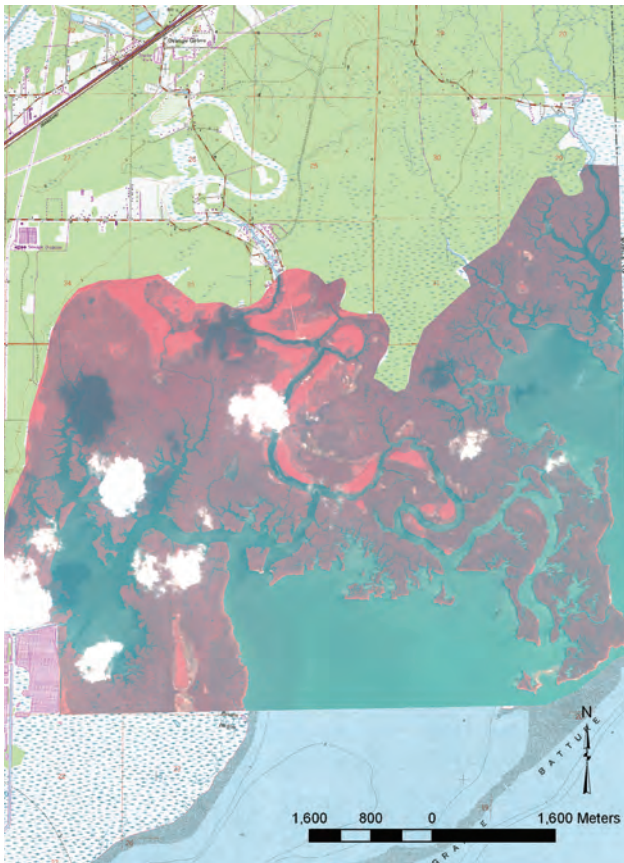

Figure 1-16. Subset of QuickBird imagery used in spectral analysis.
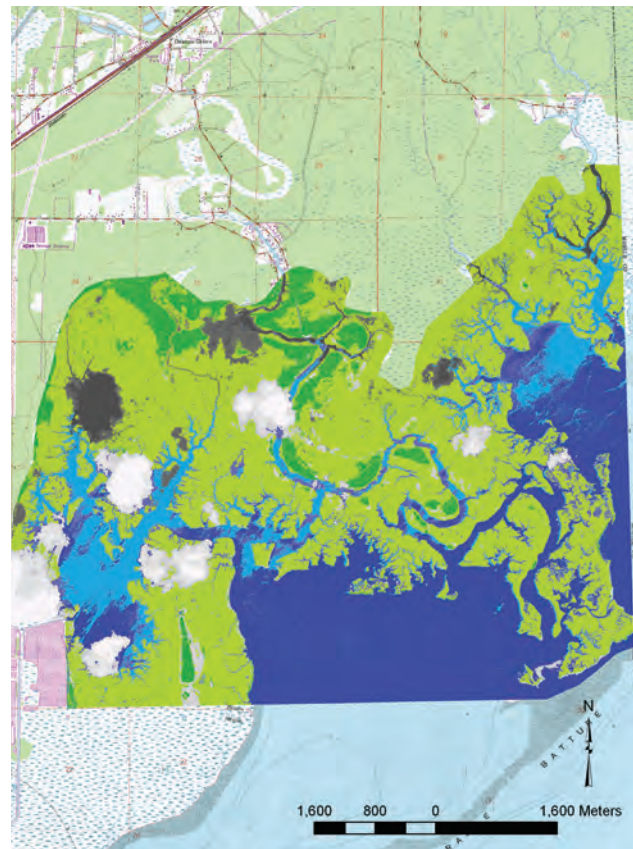

Figure 1-17. Unsupervised classification, 10-class solution.

ture, has a single class in the 10-class results, expands to two classes in the 15-class solution, and is subdivided no further in the 20-class results. Moreover, there is no identifiable relationship between either of the two hammock vegetation classes and site location. Looking at the 15-class breakdown of three sites well-situated in the hammock environment, between 87% and 97% of the pixels fall into the two hammock classes, as expected, while these classes make up less than 10% of the survey area (Table 1-2, Figure 1-20). Did the unsupervised classification produce anything that helps us differentiate hammock areas with sites from those without sites? There is no clear relationship between either hammock class and site composition. Looking only at these two classes, one predominates at one site while the other predominates at the other two sites. Variation within the hammocks is too subtle to allow us to detect site location on the basis of an unsupervised classification.

Therefore, two supervised classifications were run, one beginning with the 22JA633 location and the other focusing on the 22JA582 location. The primary focus of these analyses was to determine whether hammock vegetation that has been enriched by the shells of prehistoric middens can be distinguished

from hammock vegetation in areas where there was no prehistoric occupation. The first step in the classification was to limit analysis to those areas where live oaks and bushes grow in the marsh. Results of the 15-class unsupervised classification were used to create a mask that included only those areas interpreted to have been hammocks (see Figure 1-18). The site boundaries of 22JA633 were used as a training field, where we derived the spectral signature that best represents the included pixels.

One of the output options in EDAS is the Euclidian distance for each pixel in the area to be classified from the mean vector of the target class. This is particularly useful in evaluating the possibility of distinguishing midden areas within the hammocks. Figure 1-21 shows the distance values from the pixels that represent the hammock where 22JA633 is located. The whiter the value, the closer the pixel is to the mean vector of the group of pixels contained within the site boundary. In this case, there is no obvious difference between the pixels within the site boundary and the rest of the hammock. When the site pixels are compared statistically to the hammock pixels (Table 1-3), there is very little difference between site and hammock in terms of mean distance. The reason for this

Figure 1-18. Unsupervised classification, 15-class solution.

Figure 1-19. Unsupervised classification, 20-class solution.

is immediately evident when the standard deviation of site pixels is considered. With a mean of 3.114 and a standard deviation of 3.069, the coefficient of variation is a remarkable 98.6 percent. Spectral characteristics of 22JA633 pixels are extremely heterogeneous, even more than the 22JA633 hammock as a whole.

When the mean distance values for 22JA587 are considered, it is evident this site also cannot be distinguished from non-site hammock areas (see Table 1-3). However, since the 22JA587 area is being measured in terms of the 22JA633 signature, perhaps this is understandable. This site is further downstream, closer to the open Gulf than 22JA633, with a probable change in the kinds and proportions of plants that make up the hammock vegetation. For this reason, a second supervised classification was run, this one beginning with the 22JA587 pixels. Recall that 22JA587 is located in a hammock situated a short distance

from another hammock without shell midden. As expected, the mean spectral distance of the pixels within the 22JA587 boundary is now smaller than it was when compared to the 22JA633 signature (see Tables 1-3 and 1-4). However, they are actually less like their own signature than those from the nearby hammock. There is still considerable variation, as illustrated by the large standard deviation in both sets. The coefficient of variation for the hammock near 22JA587 actually exceeds 100 percent.

It is apparent that it will not be possible to derive a spectral signature for site locations using the four bands of the QuickBird imagery. Given the remarkable within-class variability that has become evident during the course of this analysis, it seems unlikely that imagery with a greater spectral resolution would be any more useful in developing a site signature. This is especially true since the hyperspectral satellite im-

Figure 1-20. Hammock vegetation as detected using the 15-class unsupervised classification.

Figure 1-21. Grey scale plot of Elucidian distance from mean vector for the 22JA633 pixels.

agery available commercially adds spectral resolution at the expense of spatial resolution. With the 30-m spatial resolution of the Hyperion sensor, for example, each pixel is represented by 220 bands of data, but 22JA633, one of the largest sites in the survey area, would be represented by less than seven pixels. 22J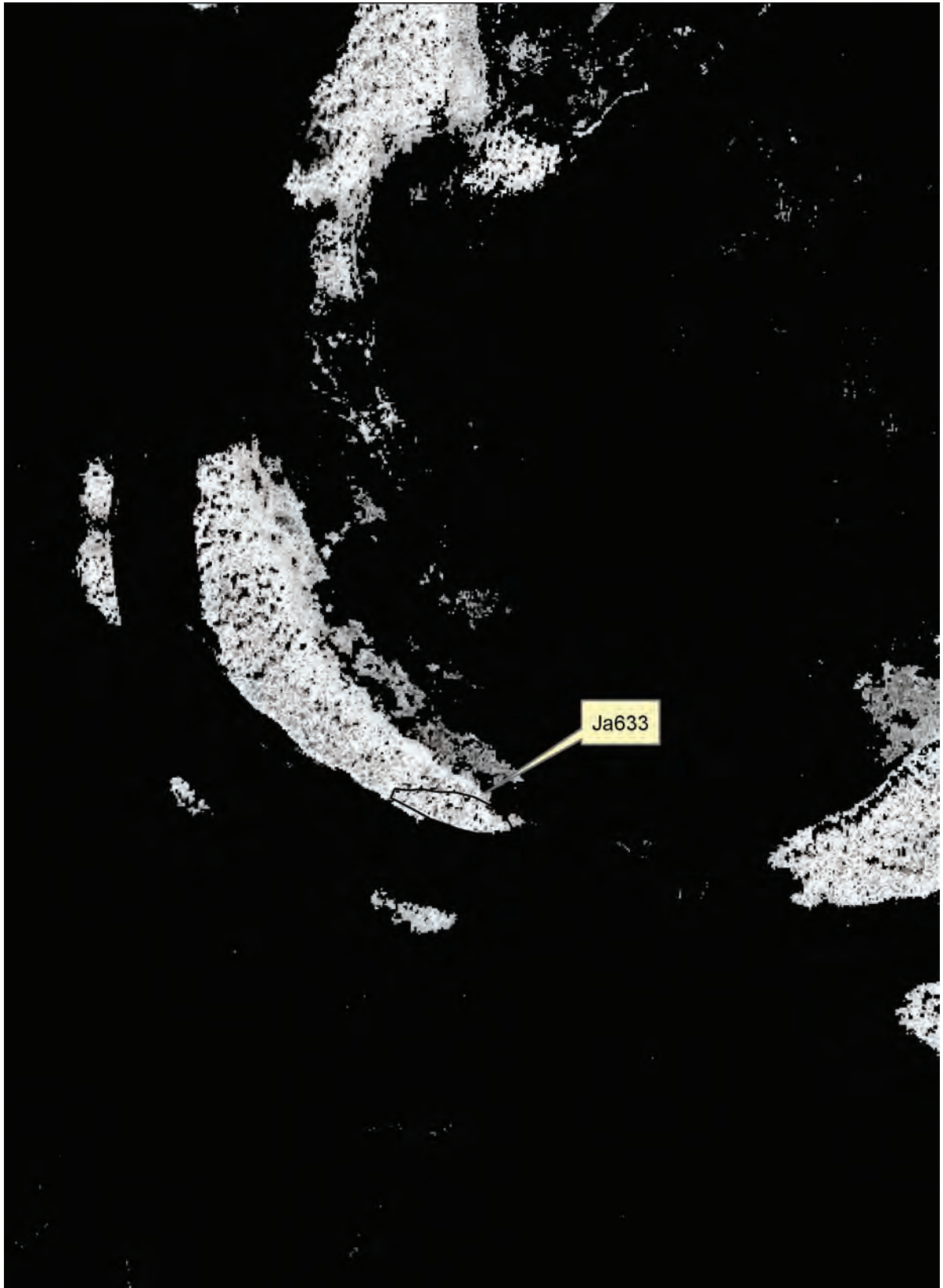A575, a more typical site in terms of size, would be covered by portions of five pixels. The relatively large footprint represented by the 30-m pixel would mask a great deal of variability.

Ground Penetrating Radar

The primary goal of the GPR survey at Grand Bay was to determine whether a boundary between shell midden and marsh sediment could be detected. Giv-

Figure 1-22. Collecting trial GPR transects at 22JA632, view to the north.

en the contrast in density between these two types of deposits, this seemed to be a reasonable objective. We hoped to be able to create a three-dimensional map of the shell deposits, allowing the total volume of the shell midden to be calculated with some accuracy.

Four sites were targeted for GPR survey: 22JA575, 22JA582, 22JA632, and 22JA633 (Figure 1-22). Test excavations were conducted at all but 22JA632, and our survey area at each site included at least some of the test units. Site 22JA632 was included in the project because, of all of the sites, this was the only one without any vegetation.

We collected GPR data along two roughly north-south/east-west survey transects during one of our early visits to the survey area. The GPR survey was conducted with a Geophysical Survey Systems, Inc. (GSSI) SIR3000 with a 400 Mhz bistatic antenna and a survey wheel. Data were collected at 32 scans per m and digitized to 403 samples per scan. Data were processed using the GPR Slice software package created by the Geophysical Archaeometry Laboratory in order to apply topographic correction to radargrams. Early results (Figure 1-23) were encouraging, with a good many high amplitude reflectors high in the profile. The boundary between the area of strong returns and relatively quiet returns dipped at the crest of the shell deposits, just as expected.

The standard technique to collect GPR data is to divide a site into 20-m or 40-m grid units and collect data along straight line transects within each unit, spacing the transects at fixed intervals, usually 50 cm. This allows data to be processed using GPR Slice to
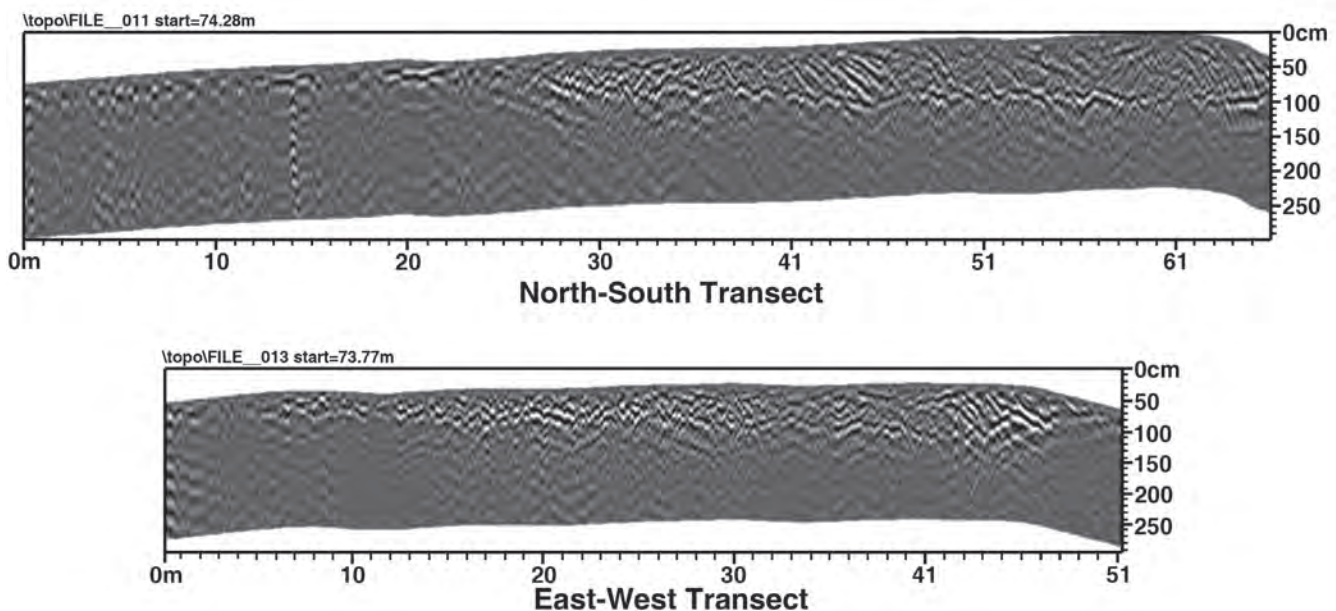

Figure 1-23. Topographically corrected trial transects from 22JA632.

create a data cube the size of the survey area on the horizontal axes and the depth of penetration of the radar signal on the vertical axis. The typical output of the program is horizontal time slices through the data cube at regular depths, as determined by calculating the speed of the signal under the specific soil conditions. We followed this procedure at all of the sites where GPR was used on this project.

However, since the radar antenna must make close contact with the ground surface in order to collect GPR data, it is necessary to clear the site of all vegetation. Site preparation often goes so far as mowing tall grass. Since it was clearly not possible to clear vegetation from the shell middens in Grand Bay National Wildlife Refuge, a different data collection strategy was developed.

The GPR system was coupled with a GPS to determine the UTM location of data being collected. Two GPS systems were used. The first, a Trimble GeoXH, recorded high-accuracy, time-stamped positions using Trimble Pathfinder software. The resulting data was post-processed to achieve location accuracies of 10 to 20 cm. The second GPS, an inexpensive Garmin eTrex, was tethered to the GPR and automatically triggered to start with the GPR. This allowed medium accuracy positions to be recorded, but, more importantly, it allowed time stamps to be recorded for each GPR scan (Figure 1-24). Data were collected by covering all of the relatively clear areas of a site with irregular and sinuous transects, walking around vegetation (Figure 1-25). Every effort was made to keep the distance between each transect less than 50 cm, to the extent that was possible given the vegetation.

In the laboratory, a special routine developed by Dean Goodman for the software package GPR Slice was used to merge the GPR, high-accuracy GPS, and medium-accuracy GPS data. Once UTM positions were determined for the data, squared amplitude time slices and 3D volumes were created. Topographic corrections were performed using data extracted from the GPS.

Since the grid was created using UTM coordinates, it was a simple matter to locate the surveyed area in the Grand Bay GIS. Although we could have used a regular grid at 22JA632, we chose to use the GPS method in order to maintain comparability between sites. When the GPR survey area for this site was superimposed on the QuickBird false color image of the south end of Bangs Island, a discrepancy was observed. When the GPR data were collected, the southern limit of the survey area was very close to the water's edge, a relationship that is not evident in the QuickBird image, but is present in a more recent Google Earth image. As it turns out, the timing of these images is critical. The QuickBird data were recorded in 2002, while the Google Earth image dates to 2007. Hurricane Katrina struck in 2005, between our two imaging events. A comparison of before-and-after images of the south end of the island shows that Katrina's storm surge not only cleared the 22JA632 shell midden of all vegetation, including what appears to be a thin covering of trees, but it also moved the shoreline at least 10 m to the north. In fact, it appeared at the time of our first visit to the site that the shell deposit at the north end of the site had been redeposited over marsh grass (see Figure 1-3).

GPR Slice was used to derive a series of amplitude slices from the 22JA632 GPR data (Figure 1-26). Each slice represents the GPR returns across about 20 cm of the vertical extent of the radar data. The slices are spaced about 14 cm apart. A color scale was applied to the data so that very strong returns were represented by red, moving through the spectrum through orange, yellow, and green to blue, which represented little to no return. If, as the trial data suggested, the boundary between shell midden and marsh deposit had been detectable, there should have been concentric bands of high (red) reflectance starting where the shell de-

Figure 1-24. Calibrating GPR and GPS at 22JA575, view to the east.

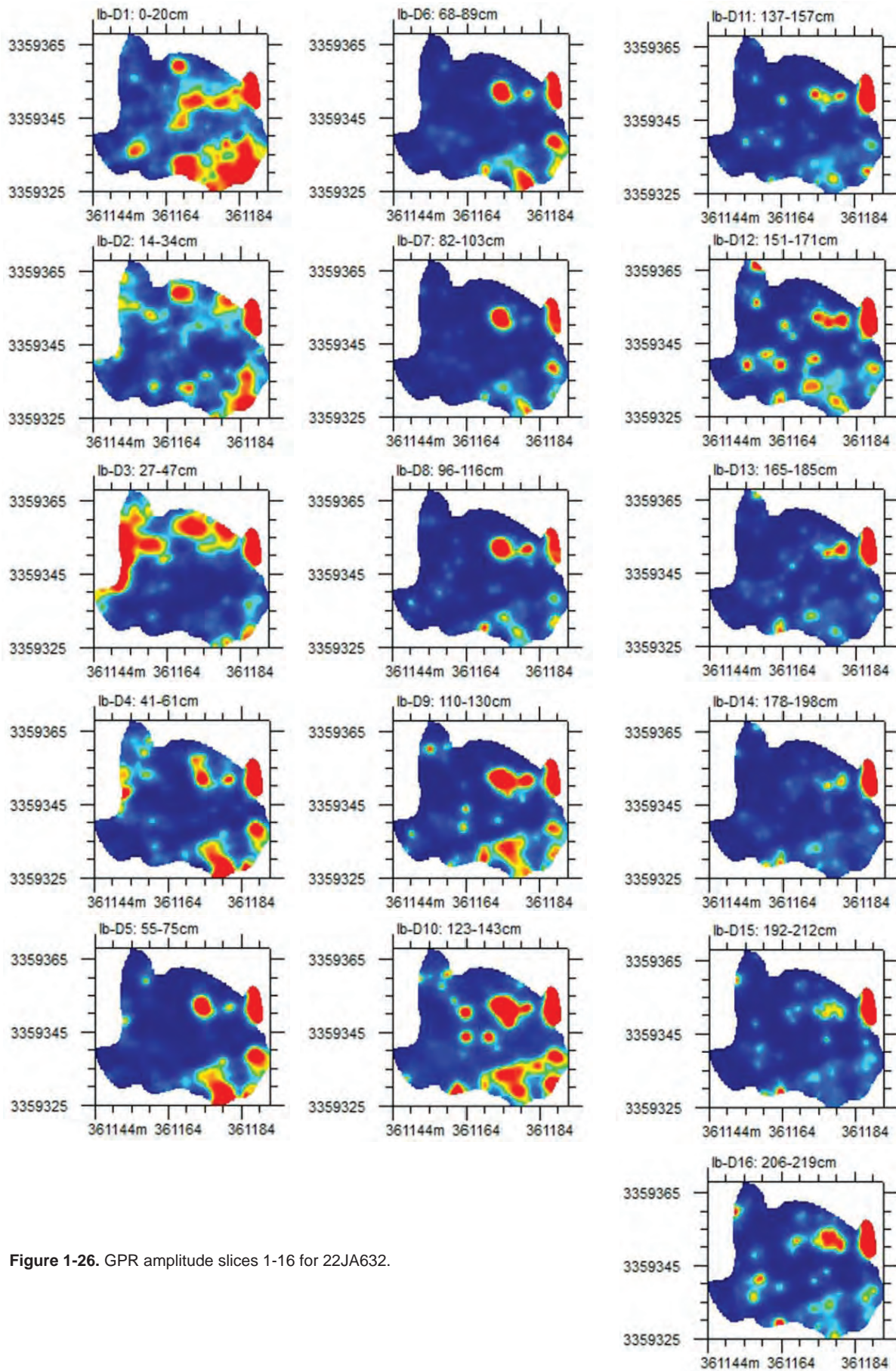**Figure 1-25**. Collecting GPR and GPS data at 22JA575, view to the west.

Figure 1-26. GPR amplitude slices 1-16 for 22JA632.

posit is thinnest and progressing toward the center, where it is deepest. Even if the deepest deposit was located somewhere else, say at the water's edge, there should have been continuous bands of reds moving in a regular pattern across the site as the depth of the amplitude slice increased. In fact there is very little patterning in the 22JA632 GPR survey data. Areas of high return tend to be small and localized, some continuing from the surface to nearly the bottom of the data, others blinking on and off with no particular pattern.

We were able to survey about a third of 22JA633, along most of the shoreline (Figure 1-27). This was also the case on all the interior sites, which had large enough open areas to get good GPR results. As we moved inland, the vegetation became denser. We used the same GPR-GPS setup and processed data in the same way, and results were similar (Figure 1-28). That is, there was no discernible pattern in the radar data and we certainly did not detect the bottom boundaries of shell middens.

We were able to survey about 20 percent of 22JA575 (Figure 1-29). There is little in those GPR slices that can be meaningfully interpreted (Figure 1-30). We covered about 15 percent of 22JA582, and once again the results were disappointing.

There are a few possible explanations for the failure of the GPR survey to detect the bottom boundaries of the shell middens. Boundaries may be irregular, with shell density decreasing gradually with depth. This is not the case at Sapelo Island, off the Georgia coast, where the boundary was well defined and clearly detected in GPR imagery (Thompson et. al 2004). Likewise, shell deposits were clearly detected in the GPR data from the Graveline Mounds, surveyed as part of this project. In both the Sapelo Island and Graveline survey areas, shells were deposited in sand. The failure of the Grand Bay GPR survey might be related to a difference in soil texture. Fine-grained sediments, such as those found in marshes, generally do not yield good GPR results (Conyers 2006:140). Alternatively, an elevated water table may have impacted our results, since it is difficult to gather radar data from saturated soils. However, if that were the case, there should have been relatively regular truncations of the data, which is not the case. Finally, perhaps too many data were lost in the GPR-GPS linkage and processing.
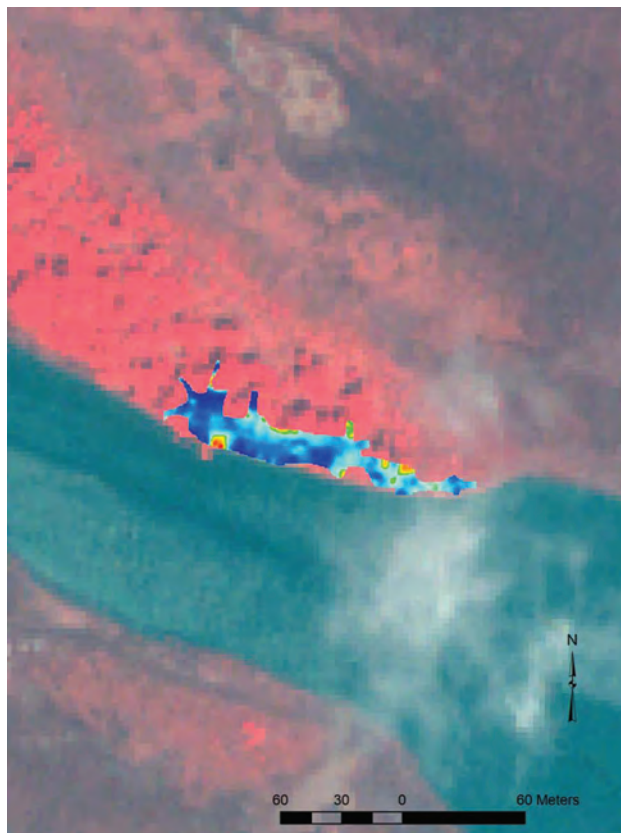

Figure 1-27. QuickBird image of 22JA633 vicinity with GPR survey results superimposed.
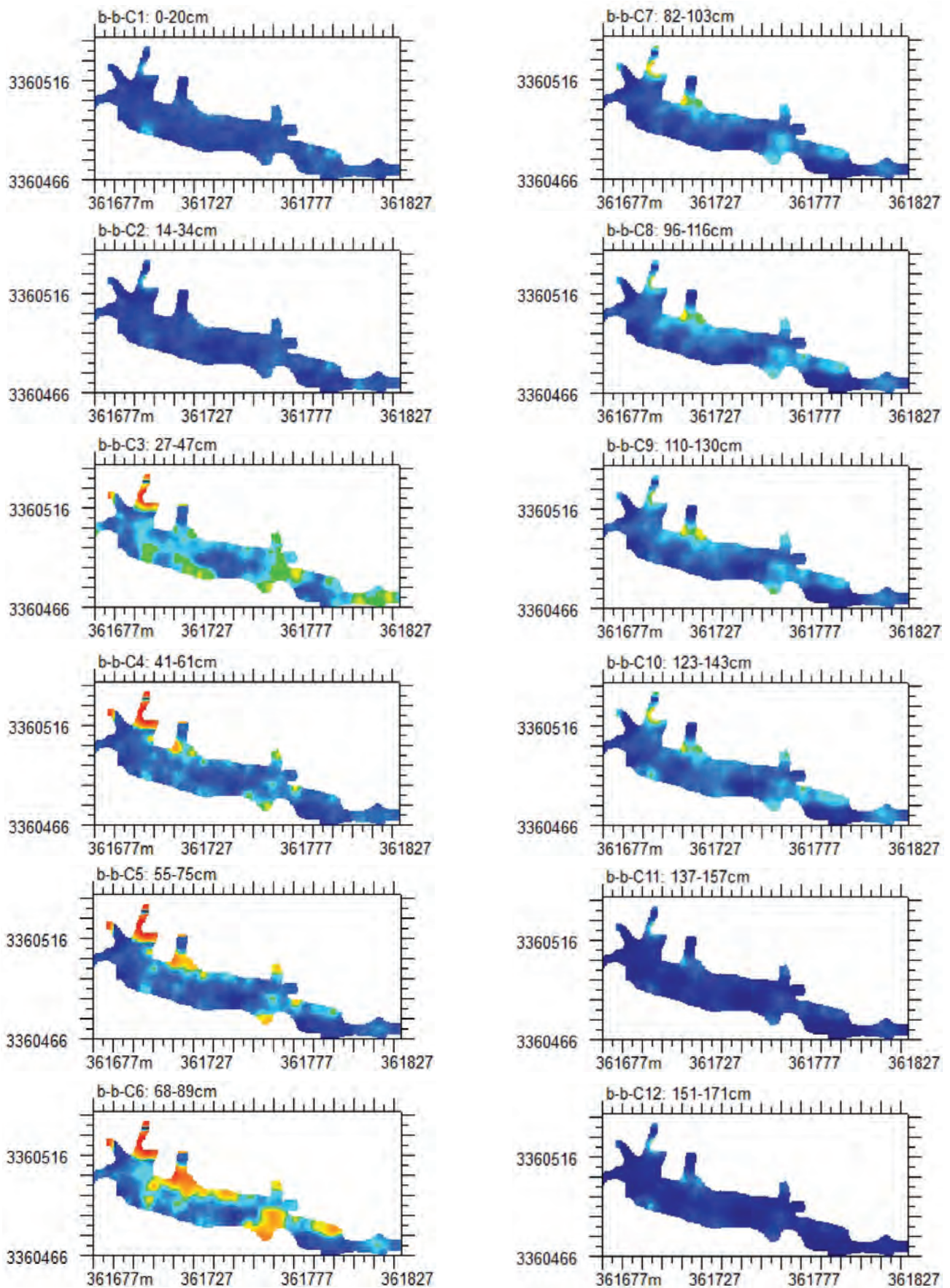
Figure 1-28. GPR amplitude slices 1-16 for 22JA633.

Conclusions

The Grand Bay remote sensing was the least successful of the four remote sensing surveys carried out as part of this project. Despite promising early results, the GPR surveys of individual sites provided nothing of use in interpreting the shell middens in Grand Bay. Dense vegetation was a problem, but even on 22JA632, swept clean by Hurricane Katrina storm surge, the vertical limits of the shell midden could not be mapped.

Likewise, our attempt to use satellite data to distinguish hammock vegetation associated with shell middens from the vegetation covering naturally occurring elevations was not successful. This may be due to the need for better spatial or spectral resolution in the satellite data. However, field observations suggest that there is, in fact, little difference between the vegetation on the elevations enhanced by shell deposits and those without shells.

The combination of remote airborne and satellite data, collected in concert with GPS data gathered in the field, was extremely useful in refining site locations. This is particularly true for some of the sites that had been recorded earlier, before GPS data was available. The GIS developed to process the Grand Bay data also allowed us to detect changes in the locations of shorelines and channels that occurred since the 1950s-era aerial surveys used to create the USGS Grand Bay SW, Miss.-Ala., and Kreole, Miss.-Ala., topographic quadrangle maps.
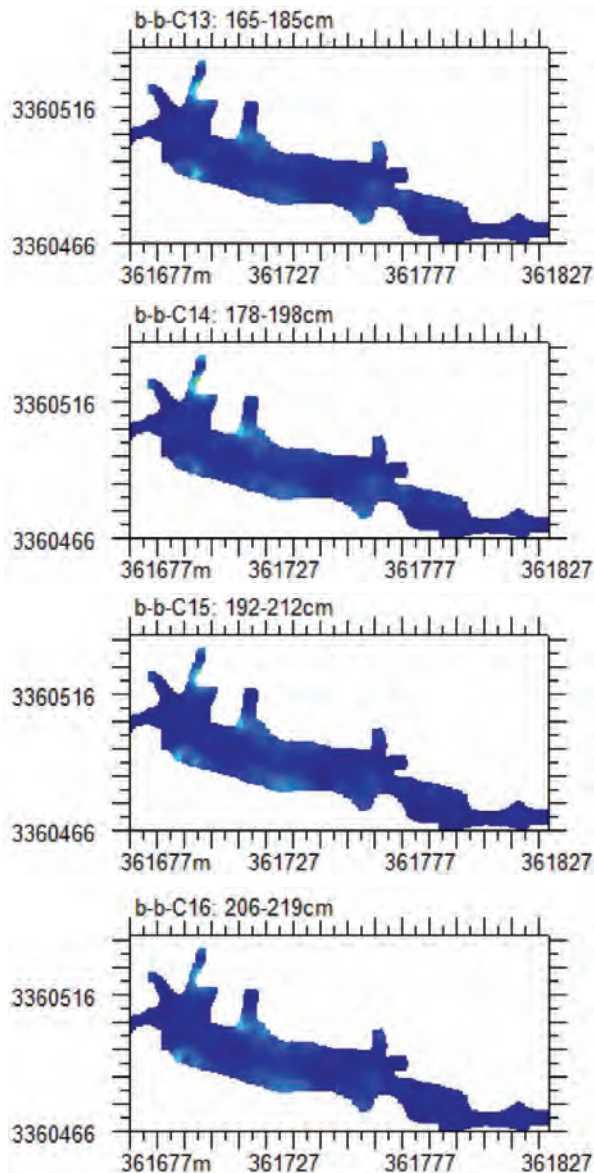

Figure 1-28 (continued). GPR amplitude slices 1-16 for 22JA633.

Figure 1-29. QuickBird image of 22JA575 vicinity with GPR survey results superimposed.
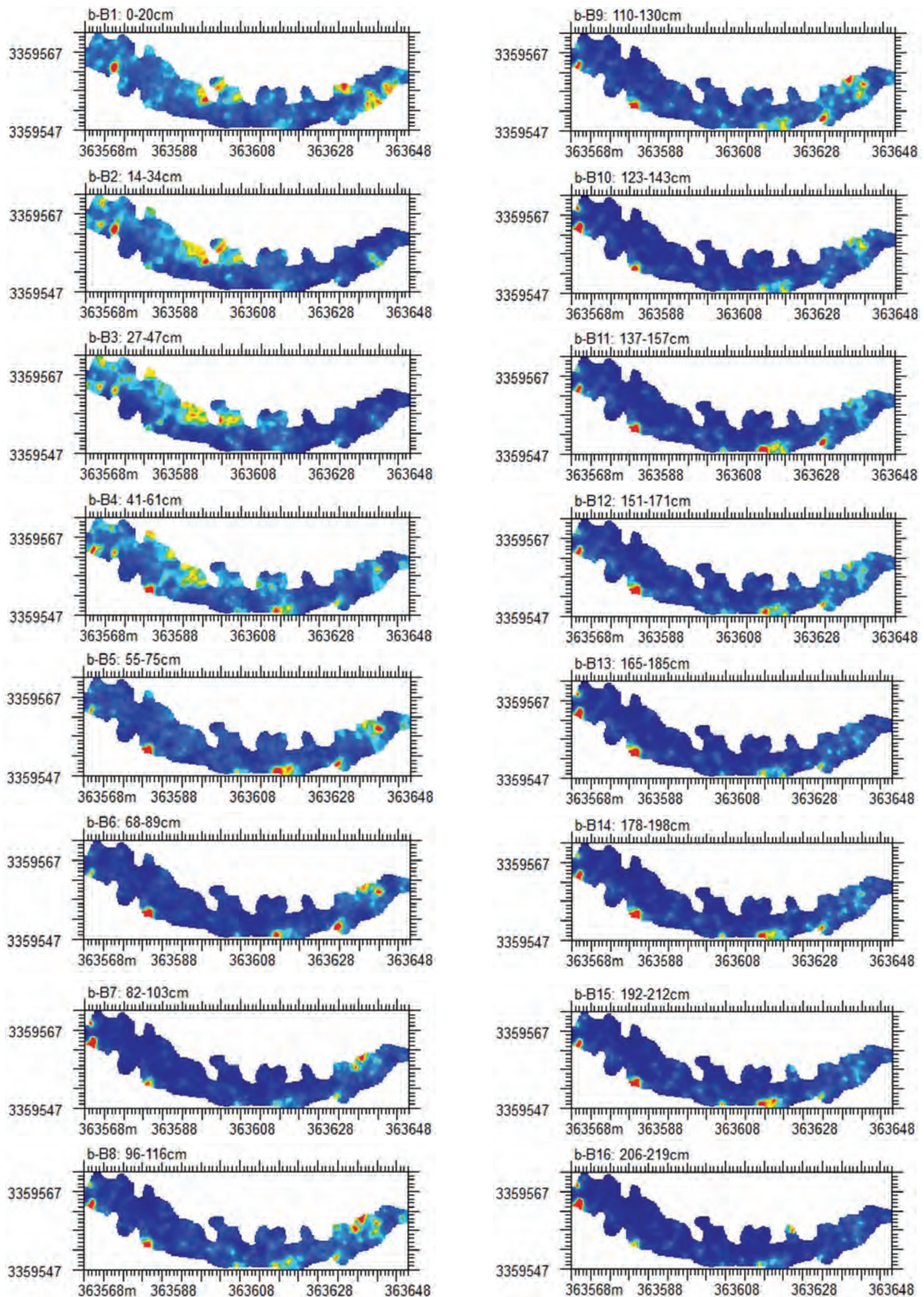
Figure 1-30. GPR amplitude slices 1-16 for 22JA575.

Fieldwork was conducted during two visits to the La Pointe-Krebs Plantation site (22JA526). The first visit during the last week of May 2010 reestablished the grid used by University of South Alabama (USA) archaeologists during their earlier investigations of the site. We also conducted gradiometer, EM, and GPR surveys. Later, after excavations were in progress, we returned to resurvey portions of the site with GPR. Our intention during the second visit was to target the limits of archaeological features (ca. 20–40 cmbs) encountered during excavations by USA archaeologists that had not been identified in data collected during the first survey.

Field Procedures

Once the site grid had been reestablished, a 20-m survey grid was laid over the entire survey area. Grid corners were marked with plastic pin flags with 20-m tapes stretched along the north and south edges of each grid block. Survey team members walked along north-south transects spaced 50-cm apart using various instruments to record subsurface characteristics of the site (Figure 2-1). Most of the property around the house was surveyed, excluding, of course, the portion covered by the La Pointe-Krebs House itself (shown in Figure 2-2 as an empty rectangle near the center of the survey area) and a portion of the property grown up in brush to the west of the La Pointe-Krebs House.

A magnetic gradient survey was conducted with a Bartington Instruments, Inc., Grad601-2 dual fluxgate gradiometer. Data were collected every 12.5 cm along transects spaced 50 cm apart. The gradiometer survey covered an area approximately 86 by 77 m. Data were processed using Geoscan's Geoplot 3.0 software.

Electromagnetic data were collected with a Geonics EM38B instrument that simultaneously records quadrature (conductivity) and in-phase (magnetic susceptibility) measurements. Readings were taken every 50 cm along transects 50 cm apart. Data were downloaded using a Geonics utility, then imported into Geoplot software for processing.

The GPR survey was conducted with a Geophysical Survey Systems, Inc. (GSSI) SIR3000 and a 400 MHz bistatic antenna with a survey wheel. Data were collected at 32 scans per m and digitized to 512 samples per scan. The time window was set to 60 nanoseconds, resulting in a maximum depth of about 2.2 m, given local soil properties. Transects were spaced 50 cm apart. Data were processed using GPR Slice software created by the Geophysical Archaeometry Laboratory. A total of 10 slices were created at a thickness of approximately 20 cm. A color palette was assigned to each slice to indicate reflection intensity.

During the second visit to the site, GPR data were collected on both sides of the USA excavation trench south of the La Pointe-Krebs House, and an additional area west of USA's excavation trench north of the La Pointe-Krebs House was surveyed. Procedures were adjusted to better detect known features in these areas.

After completion of data processing from both trips, plan view maps from excavations were overlaid onto images of the geophysical data. The map overlays accomplished in ArcGIS software indicate that many of the archaeological features encountered in excavation by USA were recorded during the original geophysical survey of the La Pointe-Krebs Plantation site. However, the long span of occupation of the site during the historic period, and the quantity of debris associated with that occupation (i.e., artifacts), make many of the intact archaeological features difficult to recognize. Pairing the plan view maps from the USA excavations and the geophysical survey allows a more detailed interpretation of the La Pointe-Krebs Plantation site.

Figure 2-1. Survey transect using gradiometer.

Survey Results

Magnetic Gradient

Gradiometer imagery shows large numbers of dipole point returns—that is, a strong negative reading located immediately north of a strong positive reading (see Figure 2-2). This kind of return indicates the locations of ferrous artifacts, a common occurrence on historic sites. Large numbers of these dipole point returns can makes it difficult to detect more subtle patterns in the data. In addition, the property is criss-crossed with utility lines, which also obscure other features on the site. Finally, the chain-link fence delineating the northern boundary of the property overpowers any weaker signals in that area. There is one anomaly of interest in this dataset, a small circular magnetic low, approximately 5 m in diameter, located south of the La Pointe-Krebs House.

Electromagnetic Induction

The EM survey of the La Pointe-Krebs Plantation site responded to the same scatter of metal artifacts and utility lines that impacted the gradiometer survey. Conductivity data depict the presence of buried utility lines across the site more clearly than the gradiometer data (Figure 2-3). The chain-link fence on the northern boundary of the property is also visible in the conductivity data, along with random low and high readings possibly related to scattered metal debris. Magnetic susceptibility data from the La Pointe-Krebs Plantation site shows only a few of the utility lines that can be seen in the conductivity data.

Magnetic susceptibility is often useful in detecting areas of relatively higher organic content, either midden or the A horizon. We hoped the shell midden deposits located at the north end of the site during the earlier shovel testing survey would be detected using this technique. They would have shown as areas of relatively higher magnetic susceptibility, but there is no such patterning in the data. Instead, there are several areas of relatively lower susceptibility, a concentration of which is located about 18 m southwest of the La Pointe-Krebs Plantation (Figure 2-4). In environments where there is a well-developed humus zone, areas of low susceptibility occur when that humus has been disturbed. That may be the case here, but the A horizon is generally poorly developed in coastal soils.

Ground-Penetrating Radar

The initial GPR survey at the La Pointe-Krebs Plantation site detected multiple high amplitude anomalies that may correlate to the early historic occupation of the site, in addition to more modern disturbances (i.e., concrete slabs, tree roots, and utility lines) that have impacted the surrounding area at varying depths (Figure 2-5). Processed data from the initial GPR survey depicts multiple long linear anomalies to the south and north of the La Pointe-Krebs House that likely represent the locations of buried utility lines (Figure 2-6). What is likely a large circular driveway shows up in the shallow slices near the south side of the property (Figure 2-7). Many clusters of high amplitude anomalies of unknown origin are scattered around the boundaries of the La Pointe-Krebs Plantation property. Unfortunately, modern disturbances obscure much of the area, which prevented features from being identified during the initial analyses of the GPR data.

After excavations were underway at the La Pointe-Krebs Plantation site, a return trip was made to re-survey portions of the site where excavations had uncovered brick foundations, pit features, and wall and fence trenches. Surveys were conducted east and west of the north-south excavation trench located south of the La Pointe-Krebs House. The GPR survey of this area was conducted using both north-south and east-west transects in order to provide overlapping data and improve the possibility of detecting subtle ar-
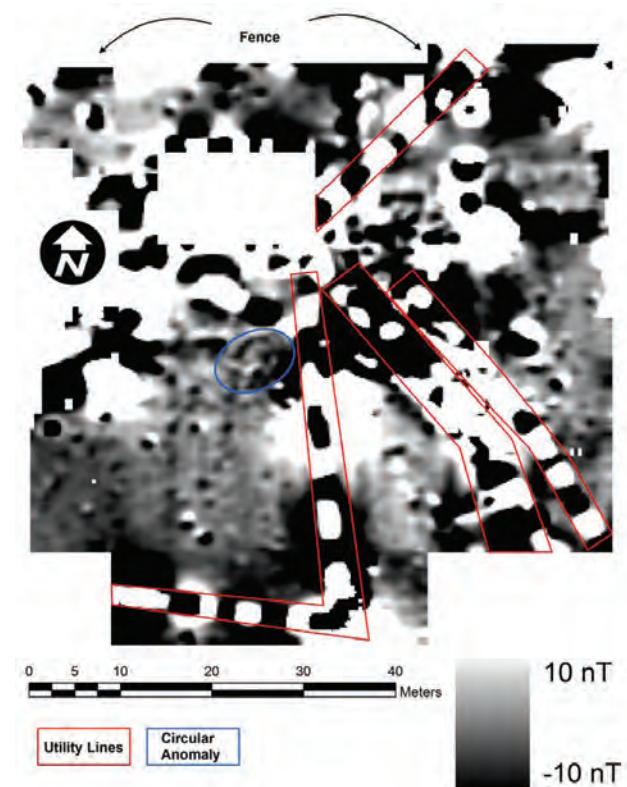

Figure 2-2. Gradiometer imagery from La Pointe-Krebs Plantation.

chaeological features. Another survey was conducted north of the La Pointe-Krebs House where excavations had uncovered double fence trenches running east-west. The original GPR survey transects in this area were run east-west, parallel to these features. The second phase survey of this area took place west of the excavation trench where these fence trenches were exposed. The survey transects were run north-south in hopes of delineating the remainder of the feature represented by the fence trenches.

The second phase GPR survey identified anomalies that could correlate to the historic occupation of the La Pointe-Krebs Plantation site. In particular, a rectangular outline can be seen south of the La Pointe-Krebs House between depths of 34 and 55 cmbs (Figure 2-8). Upon re-inspection of data from the initial GPR survey of this area, high reflection anomalies are present in this area between the depths of 41 and 61 cmbs. However, the rectilinear shape is not as clear in the first phase survey (Figure 2-9). These anomalies may represent the remains of a historic structure on the property.

The second phase GPR data from the area south of the La Pointe-Krebs House also show a circular anomaly between the depths of 51 and 72 cmbs (Figure 2-10), in the same locale as the circular anomaly evident in the gradiometer data. This area was not tested, but the circular shape of this anomaly and its appearance in two separate datasets suggest that it may be a cultural feature.

GPR results from the area north of the La Pointe-Krebs House show a high amplitude reflection that may represent a continuation of the fence trenches exposed by excavation (Figure 2-11). This lineament appears to turn south at a right angle to the west of the trench, which may mark the western side of the feature represented by the excavated fence trenches. However, once again, the results are not clear, likely obscured by the long history of habitation on the La Pointe-Krebs Plantation property.

Conclusions

The EM survey produced little information relevant to the archaeological interpretations of historic occupations at the La Pointe-Krebs Plantation site. Conductivity and magnetic susceptibility components of the EM signal primarily revealed locations of buried utility lines, in addition to scattered metal debris. The magnetic susceptibility data do depict an amorphous area of low susceptibility roughly 18 m southeast of
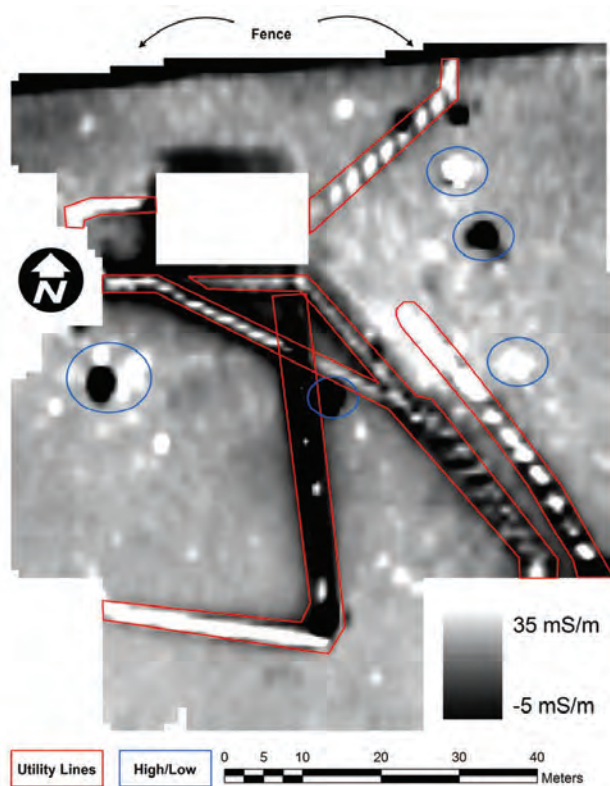

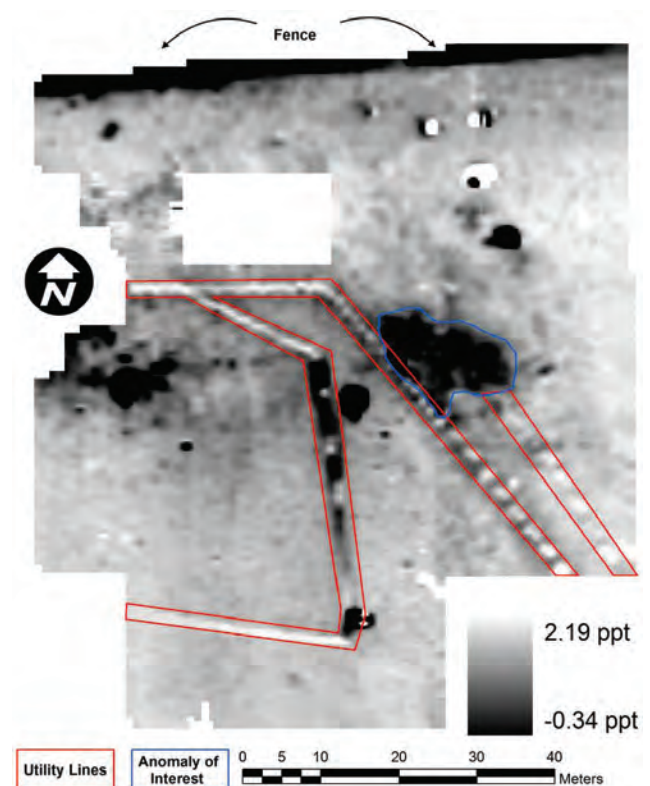**Figure 2-3.** Conductivity imagery from La Pointe-Krebs Plantation.

Figure 2-4. Magnetic susceptibility data from La Pointe-Krebs Plantation.
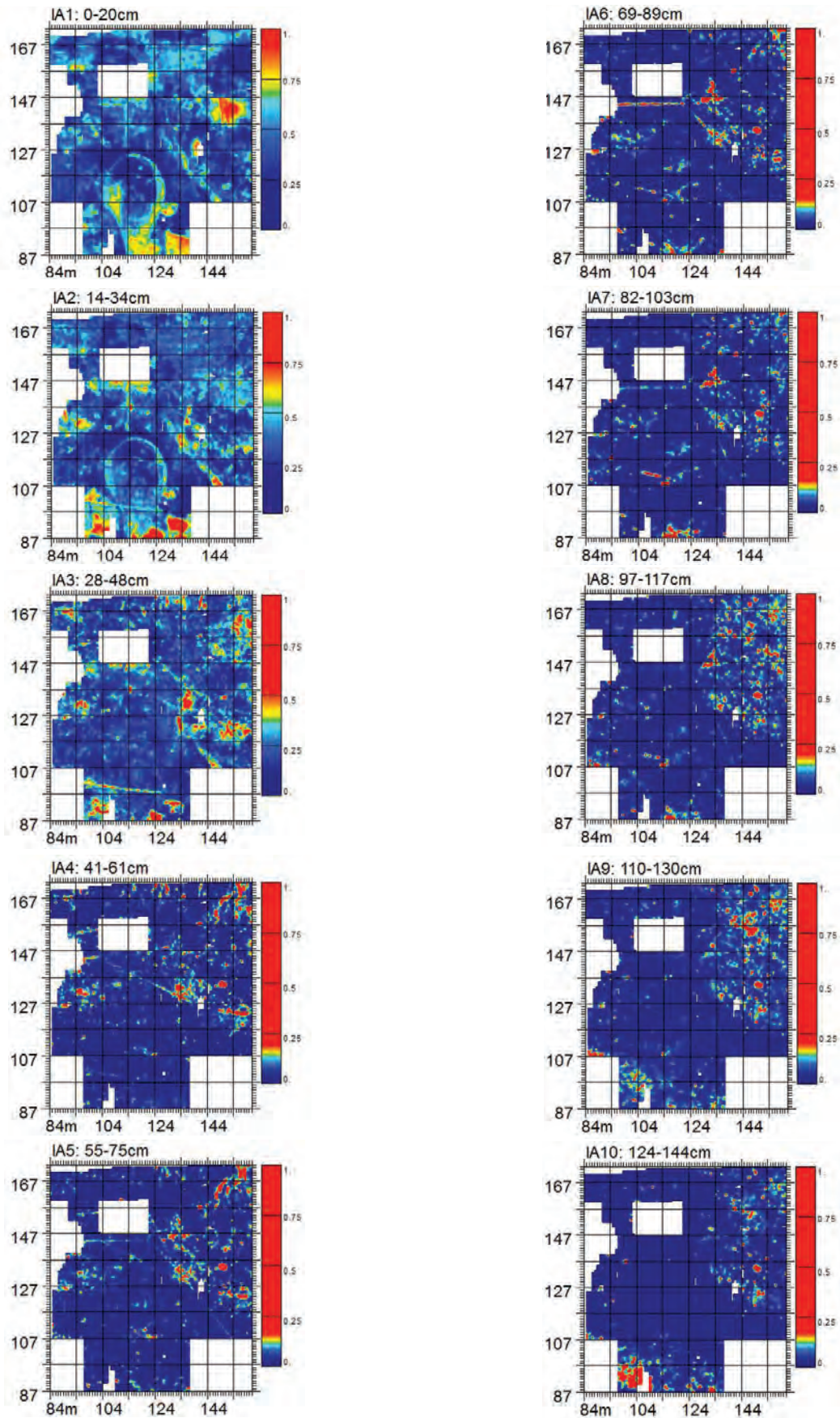
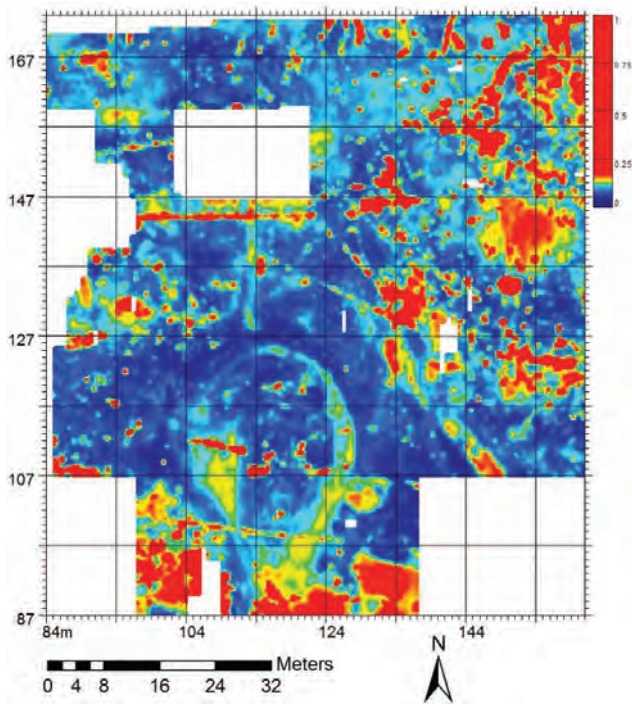**Figure 2-5.** First phase GPR amplitude slices 1-10.

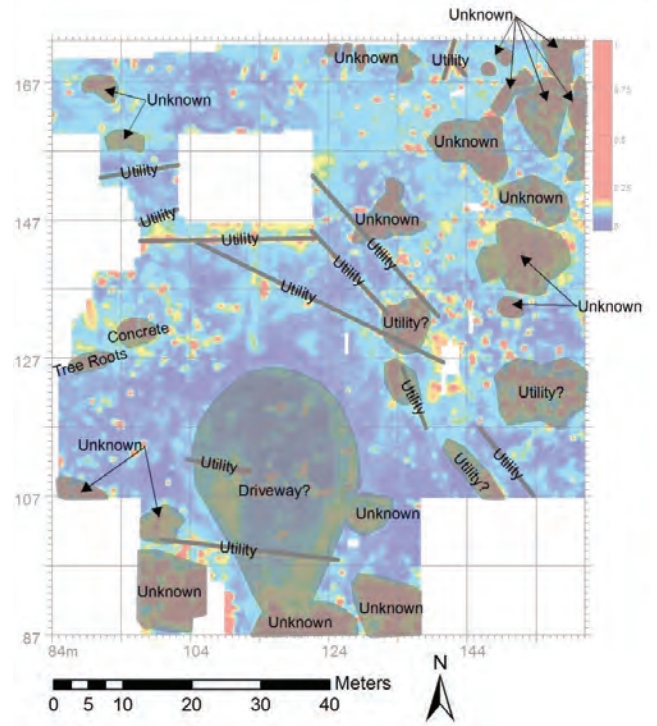**Figure 2-6.** First phase GPR overlay.

Figure 2-7. First phase GPR overlay with interpretations.
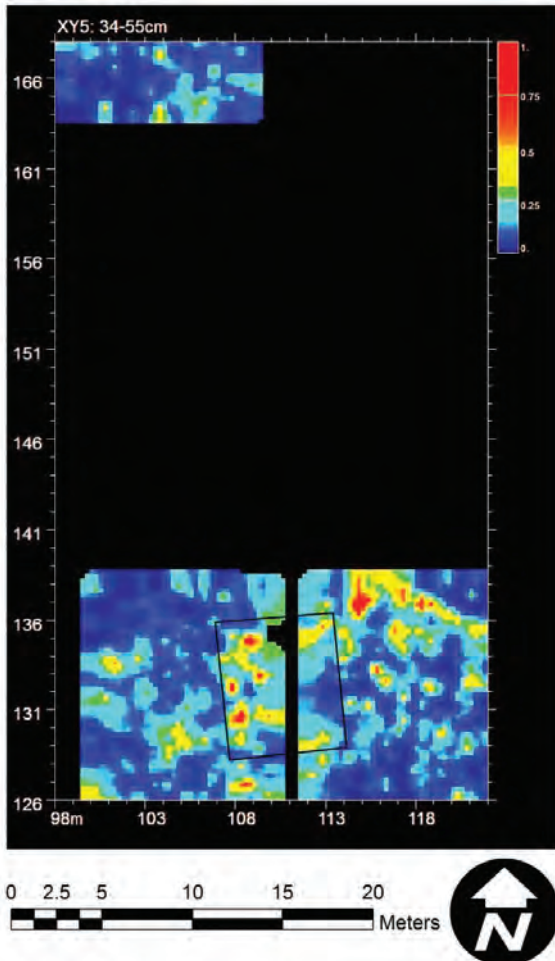

Figure 2-8. GPR data from second phase survey, rectilinear pattern outlined in black.
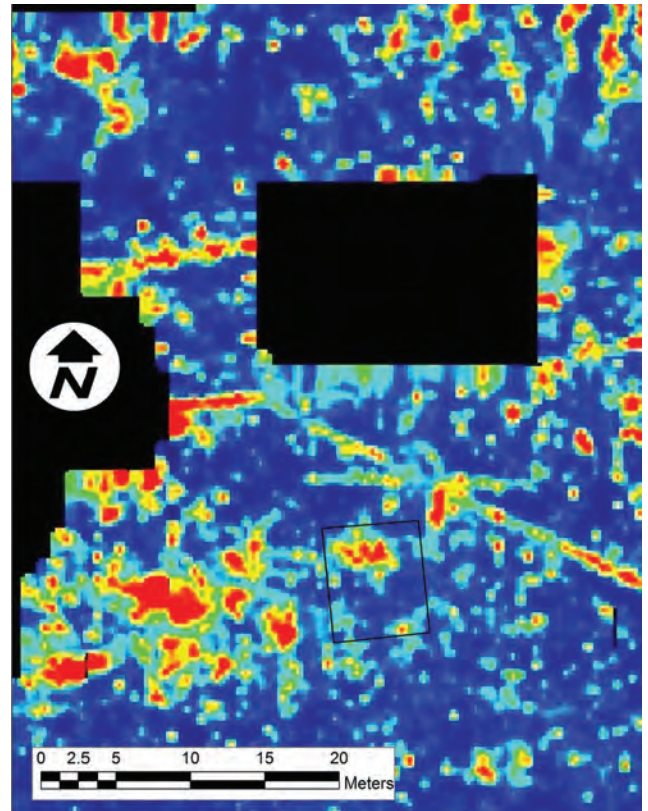

Figure 2-9. First phase GPR amplitude slice 4 (41 to 61 cmbs), enlarged to show area of interest outlined in Figure 2-8.

the La Pointe-Krebs House. This area could represent a fairly large disturbance of the A horizon. The gradiometer data show a mass of scattered metal debris in the area, perhaps indicating disposal of historic debris in that location. There is little that suggests a structure was located in this area.

The gradiometer imagery primarily shows the same metal debris and utility lines depicted in the EM data. However, a roughly circular anomaly can be seen south of the La Pointe-Krebs Plantation site. This anomaly is also present in depth slices between 34 and 72 cmbs in the GPR data. There is no apparent internal pattern to the feature in either data set.

The first phase GPR survey was initially unsuccessful in identifying cultural features dating to the early

historic occupation of the site. Utility lines, a driveway, and multiple unknown high amplitude reflections were the only anomalies identified. The second phase GPR survey that took place after excavations were underway revealed anomalies with roughly rectilinear shapes. These anomalies were not oriented with the fence trenches encountered in excavations, but their shapes suggest historic origins. Upon re-inspection of the original GPR data from the La Pointe-Krebs Plantation site, many of the anomalies found in the second phase survey were discovered in the original data. When the cultural features exposed by excavation are overlain on the GPR image (Figure 2-12), there is some correspondence between features and high amplitude reflections. However, the correspondence is not consistent, and the shapes of reflections relating to early historic features in
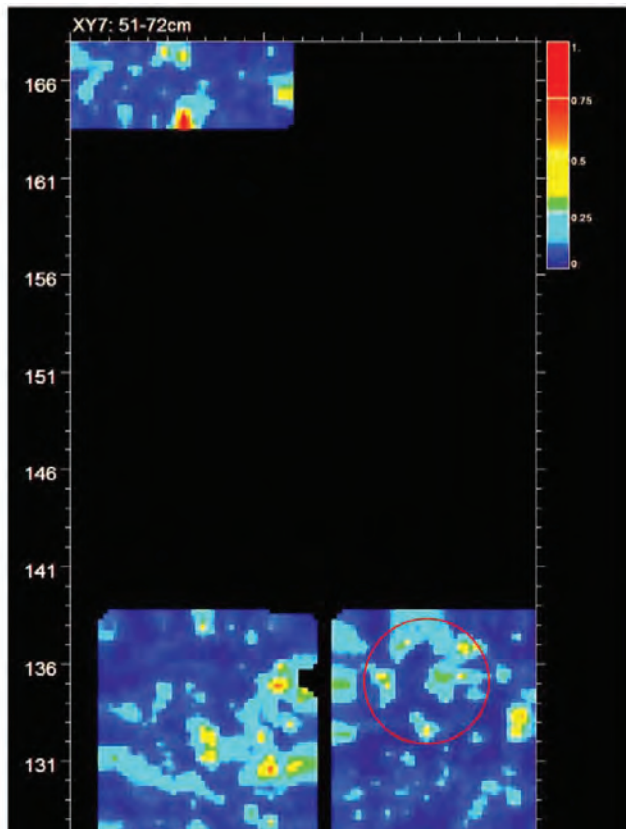

Figure 2-10. Second phase GPR data with circular anomaly in gradiometer data overlaid.
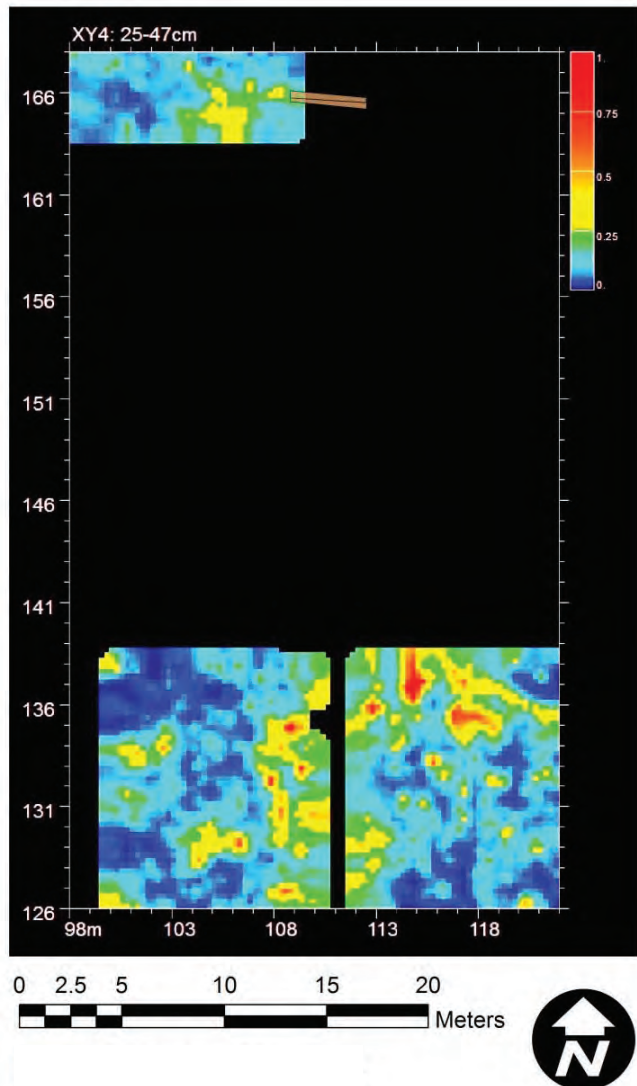

Figure 2-11. Second phase GPR data with outline of double fence trenches overlaid.

the GPR data make it difficult to differentiate these features from other features that may have resulted from later historic occupations of the site.

Going into this project, it seemed likely that the La Pointe-Krebs Plantation site would provide an ideal opportunity to apply geophysical survey techniques in delineating cultural features. The area was mostly open and planted in closely mowed grass. Sandy coastal soils are ideal for GPR survey and generally neutral in terms of magnetic characteristics. That is, magnetic disturbances are likely to be cultural. We had hoped to be able to detect the relatively subtle enhancement in magnetic susceptibility that marks the location of prehistoric midden deposits. Our recent experience at the Graveline Mound (see Chapter 4), a prehistoric site situated on soils similar to the La Pointe-Krebs Plantation site, has shown us that there was no detectable enhancement of magnetic susceptibility associated with the buried A horizon at that site. Moreover, midden deposits rich in shell and organic material in the mound fill were exposed during excavation of the mound. To our surprise, we found no elevation of magnetic susceptibility associated with these features, although they were readily detectible using GPR and resistivity tomography. There may be

little available ferruginous mineral in these relatively young soils, and the biological activity that enhances susceptibility in midden deposits in most soils may not be a factor here.

There has been a good deal of cultural activity that has left magnetic signatures at the site. Unfortunately, most of them take the form of utility lines, chain-link fences, and a broad relatively dense scatter of metal. All of these high return features expand the range of the magnetic imagery, making it difficult to detect low amplitude prehistoric and early historic features.

There were likewise a large number of reflectors in the radar imagery, many of which relate to the twentieth-century occupation of the site. Many of the historic features uncovered in the excavations were either relatively shallow or low contrast (in terms of radar) construction trenches filled with soil similar to the soil in which they were dug. Shallow features are difficult to detect because of the way in which the radar signal is transmitted into the soil. Finally, even in those instances where there was a general correspondence between remote sensing imagery and excavation results, the patterns of features revealed in the remote sensing imagery were not clear. One of the primary techniques for detecting cultural features is image recognition. Utility lines are long, narrow, continuous patterns. Driveways are shallow broad patterns. House foundations are relatively small linear patterns with right angles. Although roughly rectilinear patterns could be seen in the GPR data, once structures had been detected, they were indistinct, lost in the clutter of other reflections, prior to excavation.
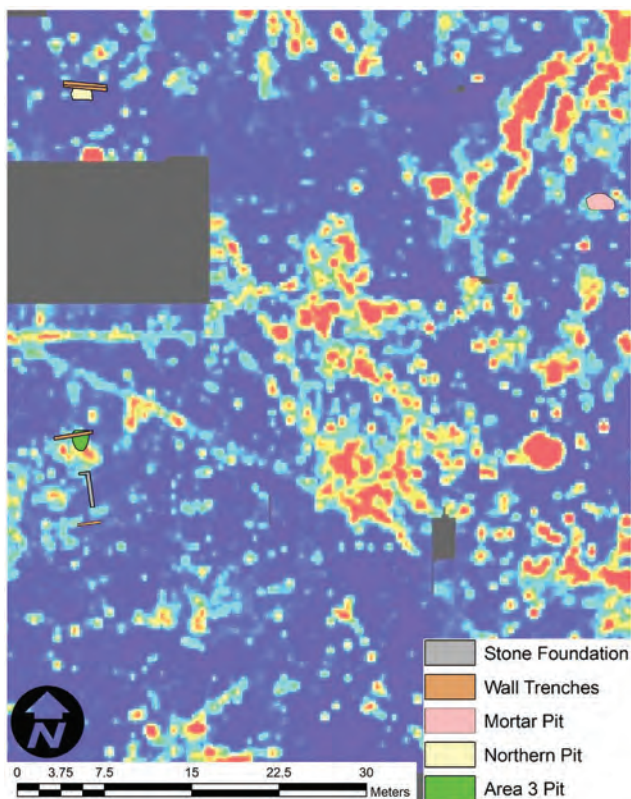

Figure 2-12. First phase GPR amplitude slice 5 (55 to 75 cmbs), enlarged showing excavation features.

Chapter 3
Jackson Landing Site

The Jackson Landing site (22HA504) is located at the extreme southwestern edge of Mississippi on the last projection of dry land before entering the Pearl River marsh (Figure 3-1). The site is grown up in hardwoods and grasses and surrounded to the south and west by marsh (Figure 3-2). Because of complications in negotiating the University of Mississippi's access to the site, we were not able to conduct our survey before the crew from East Carolina University (ECU) had completed their excavations. So, although they were not able to use our imagery to guide their excavations, we used their excavation results in targeting areas for remote sensing. As a result, we are able to make advances in our understanding of the utility of the various instruments in a coastal setting.

Two site areas were targeted by our survey (Figure 3-3): the west bluff and the mound vicinity. We did a good deal of work on the mound and just northeast of the mound, where a test pit uncovered a buried shell midden. We also conducted surveys on the west bluff of the site, where additional buried shell midden was uncovered.

Field Procedures

Geophysical investigations at the Jackson Landing site were carried out in 2010 during two visits, in late July-early August and in mid-August. During the first trip, magnetic gradient and EM surveys were performed in the bluff area, while a GPR survey was conducted on the mound. Down-hole investigation of anomalies detected at the bluff and the mound area were accomplished during the second site visit.

Magnetic gradient survey of the bluff was performed with a Bartington Instruments, Inc., Grad601-2 dual fluxgate gradiometer. However, due to uneven terrain over this portion of the site, the instrument was operated in single-sensor mode to obtain more accurate data. Data were collected every 12.5 cm along transects spaced 50 cm apart. The gradiometer survey covered an area measuring 5.5 x 14.0 m. Data were processed using Geoscan's Geoplot 3.0 software and placed in ArcGIS for final data visualization. The EM survey was conducted with a Geonics, Ltd.,

EM 38B electromagnetic induction meter. Data were collected every 0.5 m along transects spaced 0.5 m apart.

GPR survey of the mound area was conducted with a Geophysical Survey Systems, Inc., (GSSI) SIR3000 and a 400 MHz bistatic antenna with a survey wheel. Data were collected at 32 scans per m and digitized to 512 samples per scan. The time window was set to 60 nanoseconds, resulting in a maximum depth of about 3 m, given the local soil properties. Transect lines were spaced at 50 cm. Data were processed using GPR Slice software created by the Geophysical Archaeometry Laboratory. A total of 20 slices were created at a thickness of approximately 17 cm. A color palette was assigned to each slice to indicate reflection intensity.
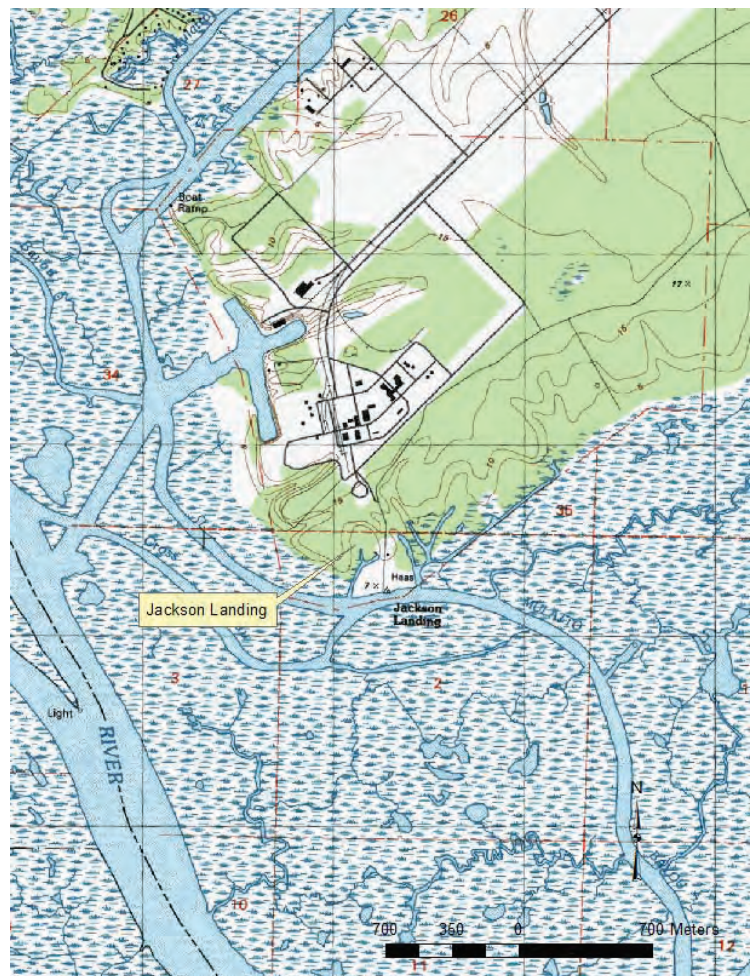

Figure 3-1. Site location (USGS topographic maps, English Lookout, Mississippi 7.5' series quadrangle).

GPR data from the mound and gradiometer and EM data from the bluff were processed before the second visit to the site. This allowed specific anomalies to be targeted for down-hole magnetic susceptibility investigations. Measurements were taken using a Bartington MS2 magnetic susceptibility meter with a MS2H down-hole probe. In areas around the mound, down-hole tests were conducted near a pit feature encountered in excavations by ECU archaeologists. First, small-diameter (2.2 cm) soil cores were removed with an Oakfield tube-sample soil core. Then data were collected in 2-cm increments down each core hole. Down-hole tests were also conducted along the trench that ECU archaeologists had excavated on the eastern flank of the mound. A total of eight down-hole tests were conducted around the mound.

Nine more down-hole tests were conducted in two areas along the west bluff. The first area was near a test unit where a shell midden was encountered by ECU archaeologists. Gradiometer and magnetic suscepti-

bility data exhibited elevated readings in this area, potentially indicating midden deposits. Down-hole tests conducted around the ECU test unit were organized in a cruciform pattern of six cores, with the distribution of cores dependent on our ability to get the core into the ground. In many areas around this test unit, the tube-sample soil core could not be forced into the ground because of shell deposits. Three more down-hole tests south of the ECU test unit were conducted to examine in-depth an anomaly present in both the gradiometer and magnetic susceptibility data. All down-hole data were processed and analyzed in Golden Software's Voxler volumetric visualization program, in addition to Microsoft Excel.

Survey Results: Mound

Ground-Penetrating Radar

The GPR survey of areas on and around the mound identified multiple high amplitude reflection anomalies. Many of these anomalies are likely associated with the modern house that once stood on the mound. Possible pipes or utility lines are visible in the 47 to 80 cmbs slice (Figure 3-4). A square anomaly is visible in the GPR data between depths of 78 and 200 cmbs (Figure 3-5). The shape and depth of this anomaly suggest that it may also relate to the house. However, the orientation of this anomaly is interesting. Instead of being oriented with the house, the square anomaly is oriented more toward the ramp of the mound. Though other high amplitude reflections are present in GPR data from the Jackson Landing mound, they do not make a distinct pattern suggestive of prehistoric cultural origins.

ECU archaeologists found a pit feature containing shells and artifacts at approximately 35-90 cmbs in a test unit northwest of the mound. GPR data from corresponding depths do not show distinct high amplitude reflections around the test unit location. However, high amplitude reflections are noted 1.0 to 1.2 m northwest of the test unit (Figure 3-6). These reflections may represent the remains of the pit feature encountered by ECU archaeologists or they may indicate the location of a separate pit feature. Alternatively, multiple small bushes were located in

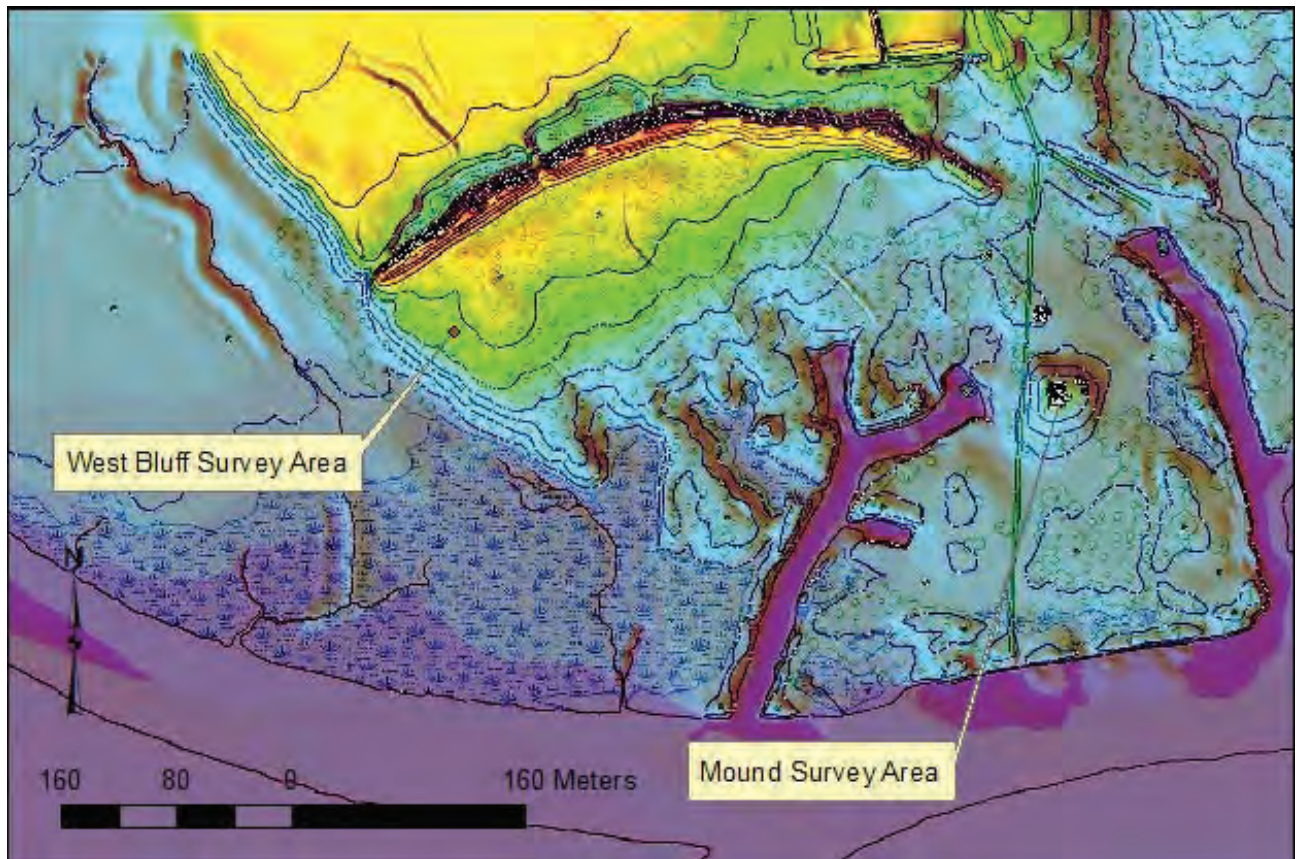**Figure 3-2.** Jackson Landing (22HA504) aerial photograph.

Figure 3-3. Geophysical survey area locations.

this portion of the survey area and it is possible that these reflections represent plant roots.

Down-hole Magnetic Susceptibility

Down-hole investigations near the mound at Jackson Landing included five cores around the test unit where the shell-filled pit was encountered by ECU archaeologists, as well as a collection of three cores placed south of an old test trench excavated on the eastern flank of the mound (Figure 3-7). Down-hole investigations around the test unit were conducted to examine the GPR anomaly detected in the area. Down-hole investigations conducted alongside the refilled test trench on the eastern flank of the mound were done in hopes of identifying a buried ground surface below the mound fill.

Cores placed around the ECU test unit northeast of the mound exhibited moderate to low susceptibility (Figure 3-8). One core exhibited a spike in susceptibility close to the surface. However, no distinct susceptibility highs were mapped within the depth-range of the GPR anomaly. The spike in magnetic susceptibility at shallow depths here is so high and confined that it may represent metal debris. The series of down-hole cores placed beside the excavation trench on the eastern flank of the mound exhibit little to no variation in

susceptibility below the mound fill. Buried A horizons usually show as a marked increase in subsceptibility reading.

Survey Results: Bluff

Magnetic Gradient

The gradiometer survey of the bluff context exhibited areas of high magnetism southeast of an ECU test unit and along the northern boundary of the survey (Figure 3-9). A large magnetic dipole is present in the south-central portion of the grid caused by a piece of roofing tin that was found buried just below the surface in this spot. Anomalies correlating with high magnetic gradient in this survey are situated at higher elevations near the top of the bluff.

Electromagnetic Induction

The EM survey of the bluff edge showed elevated conductivity at the east end of the survey area (Figure 3-10). There is a general drop in conductivity as you move down slope. High magnetic susceptibility values were also recorded at the crest of the ridge (Figure 3-11). Once one discounts the high magnetic return from the roofing tin, there is a particularly strong cor-
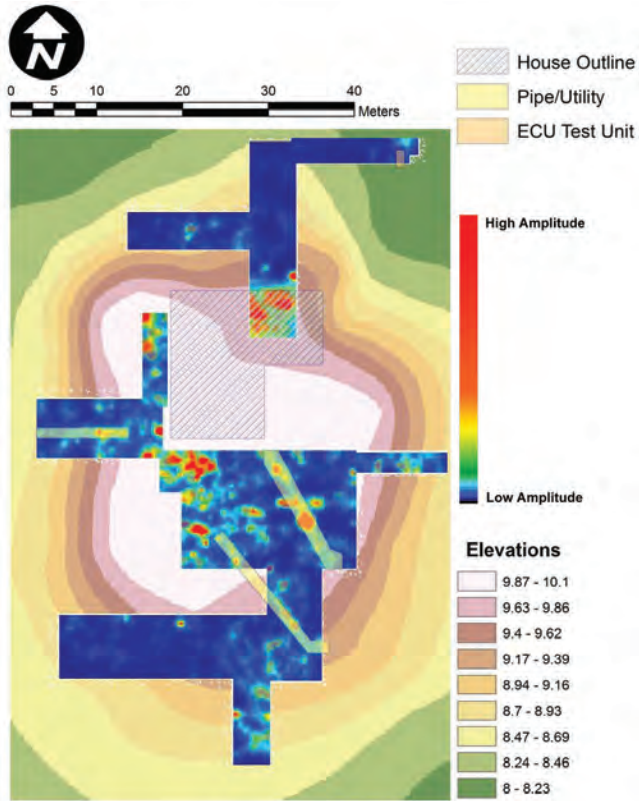
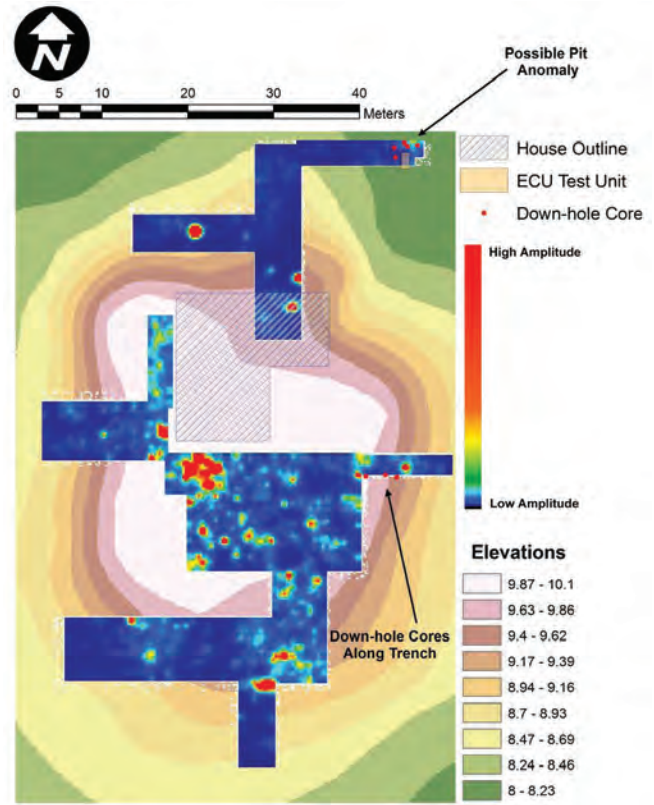**Figure 3-4.** GPR amplitude slice map for the mound, 47 to 80 cmbs.

Figure 3-6. GPR amplitude slice map for the mound, 78 to 95 cmbs.
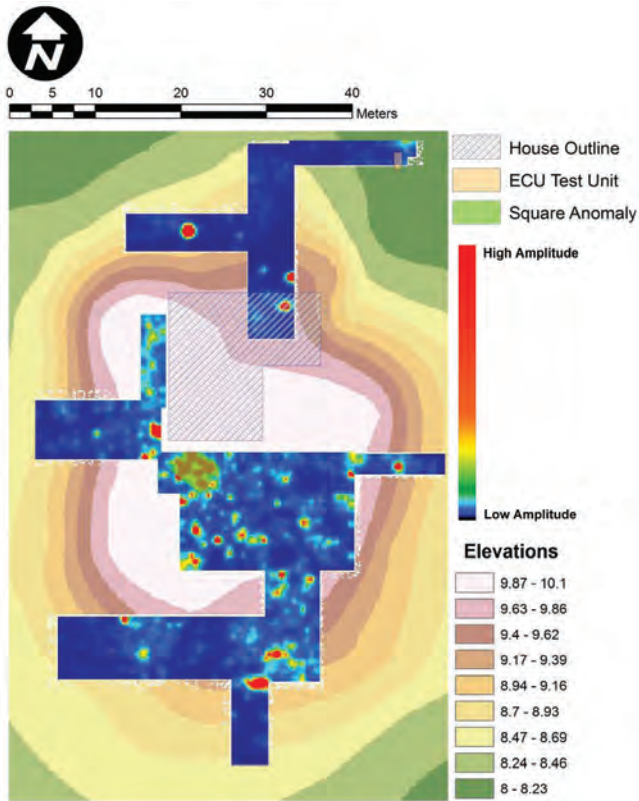

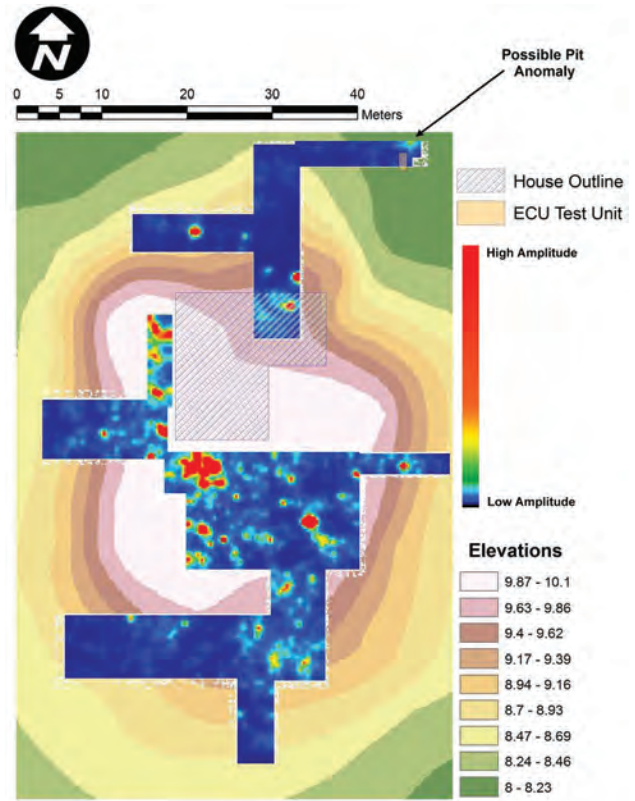**Figure 3-5.** GPR amplitude slice map for the mound, 93 to 111 cmbs.

Figure 3-7. GPR amplitude slice map for the mound, 93 to 111 cmbs, down-hole cores locations marked.

relation between areas of high return in the magnetic gradient image and the magnetic susceptibility image. This is exactly the kind of correspondence we have come to associate with midden deposits on prehistoric sites in northern Mississippi.

Down-Hole Magnetic Susceptibility

Data were collected from nine down-hole cores placed over possible midden-like anomalies identified in the gradiometer and EM surveys (Figure 3-12). Six cores were placed in a cruciform pattern north of the ECU test unit, and three more were located along the northern edge of the geophysical survey area on the bluff. It was difficult to take cores at the bluff due to the dense shells in the midden deposits there. Cores located near the test unit showed relatively high susceptibility readings concentrated near the edge of the survey area (Figure 3-13). Cores along the northern boundary of the survey area exhibit high susceptibility throughout (Figure 3-14). In both cases, down-hole results corroborate the magnetic gradient and EM results. The instruments were able to detect buried midden deposits along the bluff edge.

Conclusions

GPR surveys in the coarse sands of the Gulf coast are generally quite informative and we got good response from the GPR survey of the mound at Jackson Landing. Unfortunately, almost everything we see in the imagery relates to twentieth-century occupation of the mound. Although multiple anomalies were identified in the GPR survey, most probably relate to construction of the modern house. The square
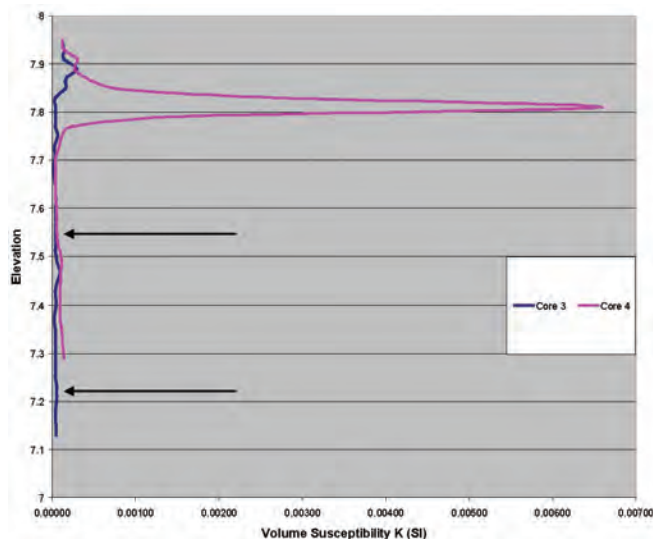

Figure 3-8. Magnetic susceptibility profiles from two cores located at the edges of ECU test unit northeast of the mound.

anomaly is most likely historic, although its orientation does not align with the concrete slab that marks the former location of the house. One GPR anomaly that may represent a subsurface pit feature is located northeast of the ECU test unit, where a shell-bearing pit was encountered during excavation. Down-hole investigations of this anomaly were inconclusive; there was no elevation in magnetic susceptibility at the depth indicated by GPR. In addition, cores placed in an east-west transect adjacent to an old test trench on the eastern flank of the mound did not detect the pre-mound buried ground surface known to be present.

The gradiometer and EM surveys of the bluff area of the Jackson Landing site suggest that midden deposits extend well outside the boundaries of the test unit excavated by ECU archaeologists. Down-hole investigations at this portion of the site reinforce this interpretation. Cores placed near the test unit and along the northern boundary of the survey area were hard to remove due to the density of shells in the bluff midden. In addition, cores placed close to the top of the bluff exhibit susceptibility highs extending deeper into the ground. This suggests that midden deposits may be more substantial on the higher elevations of the bluff.

The success of the magnetic susceptibility surveys, both EM and down-hole, at the bluff area is all the more significant because similar surveys conducted at the Graveline Mound and the La Pointe-Krebs Plantation site were unsuccessful. In fact, pockets of shell midden with associated dark black organic deposits were exposed in the excavation units at Graveline Mound and their extents mapped using GPR and resistivity tomography, yet they could not be detected using down-hole susceptibility. Neither was it possible to measure an increase in magnetic susceptibility using a hand-held KT-9 susceptibility meter to take readings of the midden exposed in the profiles of the trenches at Graveline Mound.

Why does the midden along the bluff edge at Jackson Landing show an elevated magnetic susceptibility, when a visually identical midden at the Graveline Mound does not? The key to that conundrum may be soils. Both the La Pointe-Krebs Plantation site and the Graveline Mound site are located on soils mapped as Wadley Loamy Sand, which is described as excessively drained. The southern third of the La Pointe-Krebs site is mapped as Harleston Fine Sandy Loam, which is described as moderately well drained. On the other hand, the entire Jackson Landing site is mapped as Escambia Loam (Figure 3-15), a relatively finer-grained soil described as somewhat poorly drained. Maybe the processes that enhance magnetic susceptibility in
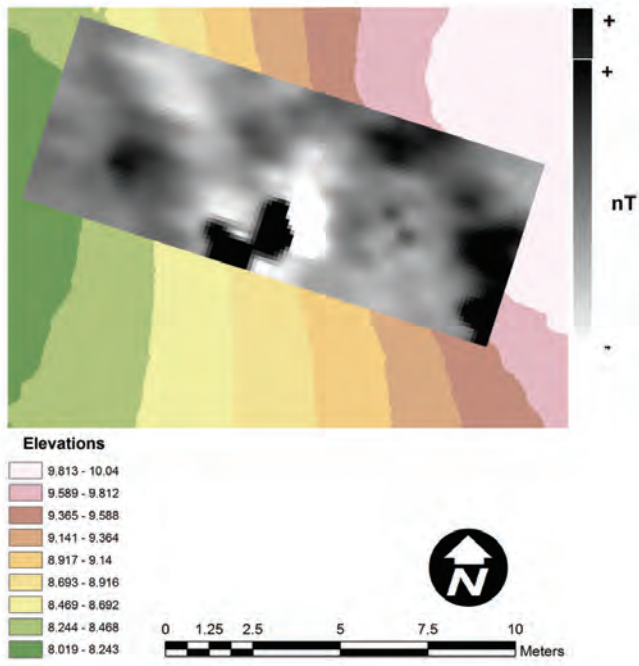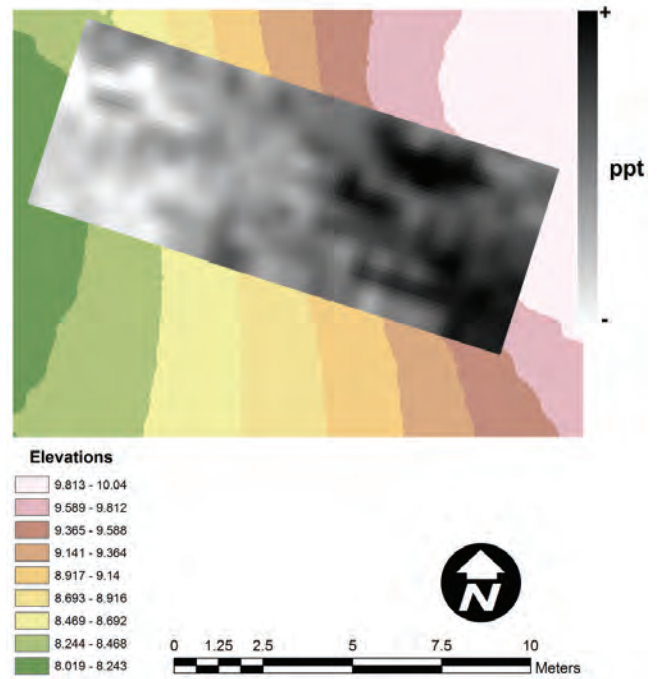
Figure 3-9. Gradiometer imagery from bluff edge.

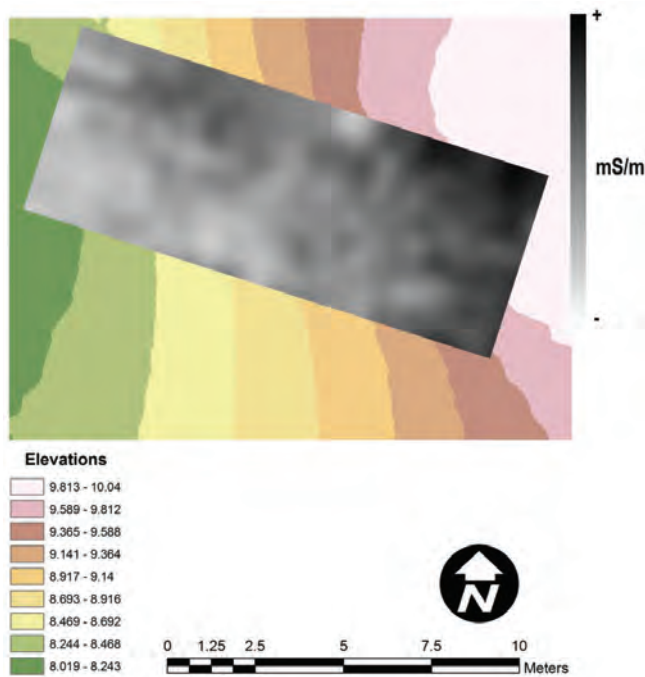**Figure 3-11.** Magnetic susceptibility imagery from bluff edge.

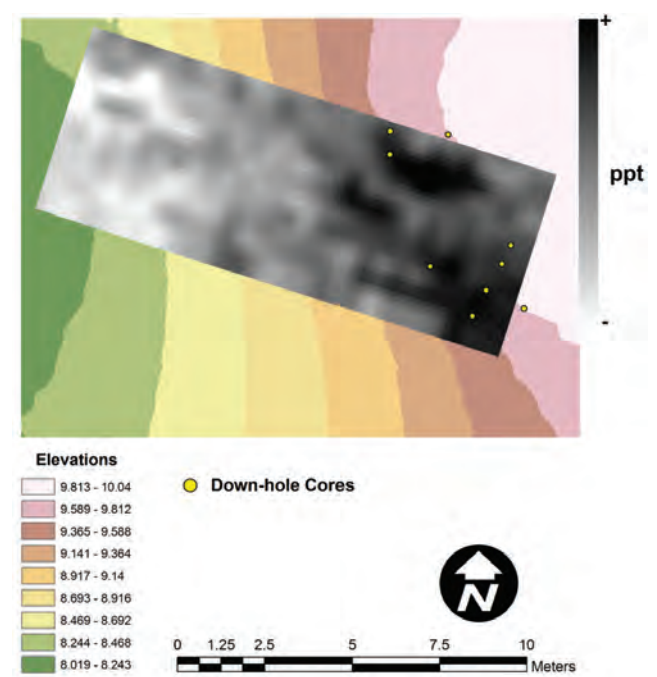**Figure 3-10.** Conductivity imagery from bluff edge.

Figure 3-12. Magnetic susceptibility, topographic, down-hole susceptibility sampling locations from the bluff edge.

rich organic deposits do not operate in well-drained soils. Or, if they do, the elements that become magnetically enhanced are leached out. Certainly our positive results in detecting midden-filled pits on Chickasaw sites in northeast Mississippi and late prehistoric sites in the Yazoo Basin support this conclusion. The soils there are fine grained and slow draining compared to the sands at Graveline Mound and the La Pointe-Krebs Plantation.
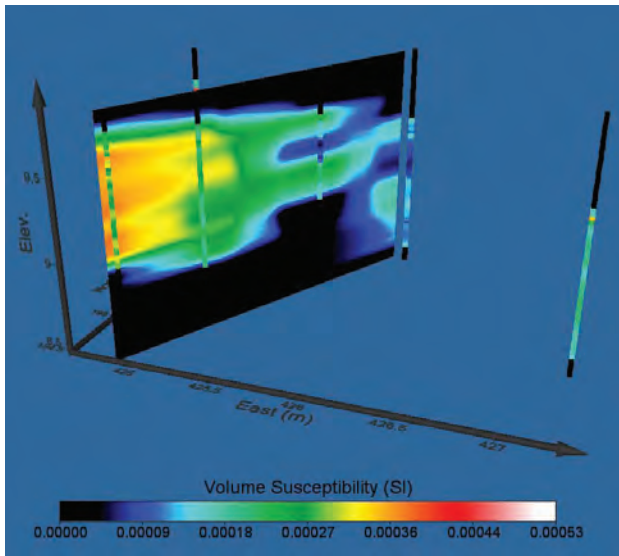

Figure 3-13. Down-hole magnetic susceptibility gradient plotted on the basis of the eastern group of cores at the bluff edge.
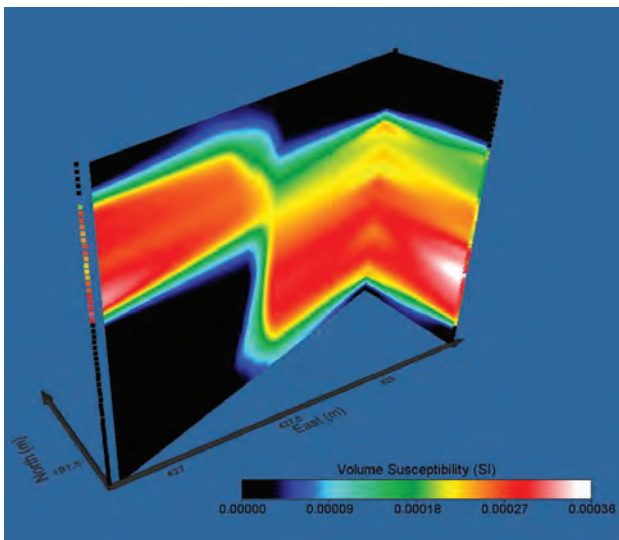

Figure 3-14. Down-hole magnetic susceptibility gradient plotted on the basis of the western group of cores at the bluff edge.
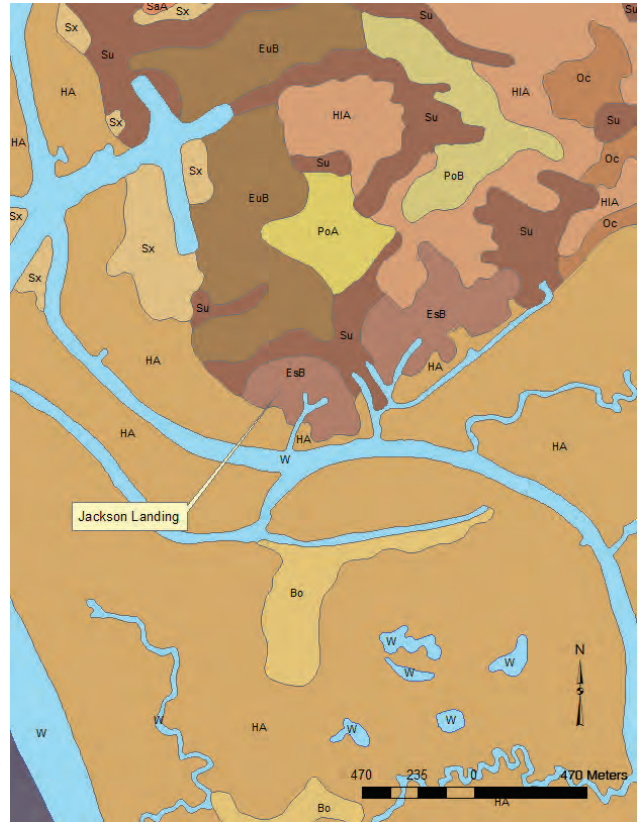

Figure 3-15. Soils mapped in the Jackson Landing vicinity.

References Cited

Blitz, John H., and C. Baxter Mann, Jr.
1993   *Archaeological Investigation in Coastal Jackson County, Mississippi.* Mississippi Gulf Coast Archaeological Project, Bay Saint Louis.

Boudreaux, Edmond A., III
2008   Archaeological Testing of the Jackson Landing Platform Mound. Paper presented at the 43rd Annual Meeting of the Mississippi Archaeological Association, McComb.
2009   *A Post-Hurricane Katrina Archaeological Site-Assessment Survey Along the Mississippi Gulf Coast.* Submitted to the Historic Preservation Division, Mississippi Department of Archives and History and the Transitional Recovery Office, Federal Emergency Management Agency, US Department of Homeland Security, Coastal Environments, Inc. Biloxi, MS.

Conyers, Lawrence B.
2006   Ground-Penetrating Radar. In *Remote Sensing in Archaeology: An Explicitly North American Perspective,* edited by Jay K. Johnson, pp. 131-160. University of Alabama Press, Tuscaloosa.

Giardino, Marco, and Bryan S. Haley
2006   Airborne Remote Sensing and Geospatial Analysis. In *Remote Sensing in Archaeology: An Explicitly North American Perspective,* edited by Jay K. Johnson, pp. 47-78. University of Alabama Press, Tuscaloosa.

Gums, Bonnie
1996   *Archaeological Survey of Old Spanish Fort Park, Pascagoula, Mississippi.* Center for Archaeological Studies, University of South Alabama, Mobile.

Henry, Edward R.
2011   A Multistage Geophysical Approach to Detecting and Interpreting Archaeological Features at the LeBus Circle, Bourbon County, Kentucky. *Archaeological Prospection* 18(4):231-244.

Hinks, Stephen, Jennifer Cohen, C. Baxter Mann, Ralph Draughon, Jr. Paul V. Heinrich, and William P. Athens
1993   *Archaeological Testing at the La Pointe-Krebs Plantation (Old Spanish Fort), Pascagoula, Mississippi.* R. Goodwin and Associates, Inc., New Orleans, LA.

Johnson, Jay K.
2006   A Comparative Guide to Applications. In *Remote Sensing in Archaeology: An Explicitly North American Perspective*, edited by Jay K. Johnson, pp. 305-320. University of Alabama Press, Tuscaloosa.

Otvos, Ervin G., and Marco J. Giardino
2004   Interlinked Barrier Chain and Delta Lobe Development, Northern Gulf of Mexico *Sedimentary Geology* 169(1):47-73.

Thompson, Victor D., Matthew D. Reynolds, Bryan Haley, Richard Jefferies, Jay K. Johnson, and Laura Humphries
2004   The Sapelo Shell Rings: Remote Sensing on a Georgia Sea Island. *Southeastern Archaeology* 23(2):192-201.

Waselkov, Gregory A., and Diane E. Silvia
1995   *Archaeology at the Krebs House (Old Spanish Fort), Pascagoula, Mississippi.* Archaeological Monograph 1. Center for Archaeological Studies, University of South Alabama, Mobile.

Weinstein, Richard A.
2009   *Jackson Landing/Mulatto Bayou Earthwork (22Ha 504/515), Hancock County, Mississippi: Past Research and Future Directions at an Archaeological Treasure.* Coastal Environments, Inc., Baton Rouge, LA.

Williams, Mark
1987   *Archaeological Excavations at the Jackson Landing/Mulatto Bayou Earthwork.* Archaeological Report No. 19. Mississippi Department of Archives and History, Jackson.